Ecological Informatics 99 (2026) 103924

Contents lists available at ScienceDirect

Ecological Informatics

journal homepage: www.elsevier.com/locate/ecolinf

Odontocete strandings from space: Accurately counting individuals with very high-resolution optical and synthetic aperture radar satellite imagery

Penny J. Clarke [a,b,*], Hannah C. Cubaynes [a], Karen A. Stockin [c,d], Ellen Bowler [a], Kris Carlyon [e], Marie R.G. Attard [a], Peter T. Fretwell [a], Aliaksandra Skachkova [a], Asha de Vos [f,g], Kaitlin M. McConnell [h], Encarni Medina-Lopez [b], Sergio Lopez Dubon [b], Jennifer A. Jackson [a]

[a] British Antarctic Survey, High Cross, Madingley Road, Cambridge CB3 0ET, United Kingdom
[b] University of Edinburgh, King's Buildings, Thomas Bayes Road, Edinburgh EH9 3FG, United Kingdom
[c] Cetacean Ecology Research Group, School of Natural Sciences, Massey University, Auckland, New Zealand
[d] Animal Welfare Science and Bioethics Centre, School of Veterinary Science, Massey University, Palmerston North, New Zealand
[e] Marine Conservation Program, Department of Natural Resources and Environment Tasmania (NRE Tas), Tasmanian Government, 134 Macquarie St, Hobart, TAS 7000, Australia
[f] Oceanswell, Colombo, Sri Lanka
[g] UWA Oceans Institute, University of Western Australia, Crawley, WA, Australia
[h] Estación Científica Fundación San Ignacio del Huinay, Fiordo Comau, Región de Los Lagos, Chile

ARTICLE INFO

Keywords:
Cetacean stranding
Dolphin
Marine conservation
Satellite remote sensing
Synthetic aperture radar
VHR satellite imagery

ABSTRACT

Cetacean strandings provide early warning of emerging concerns regarding animal, ocean, and human health and allow insights into local cetacean population, density, distribution and mortality, and thus offer significant conservation value for the assessment of ecosystems. However stranding networks (programmes for monitoring and coordinating a ground response and investigation of local strandings) are infrequent to non-existent within minimally populated areas, coastal areas with limited economic resources, geographically remote areas, complex coastlines and areas of geopolitical unrest. Very high-resolution (VHR) satellite imagery offers the prospect of improving monitoring in these regions. While VHR optical satellite imagery is able to detect large baleen whale strandings (> 12 m), mass strandings (MSE, strandings of two or more animals excluding mother calf pairs) are predominantly of smaller-sized odontocetes (∼1–6 m). Detecting odontocetes is therefore crucial for VHR satellites to be useful for monitoring strandings globally. Here, we analyse MSEs involving large (∼11–18 m) and small odontocetes to; (1) investigate whether stranded animals can be detected and counted in VHR optical satellite imagery, (2) determine the minimum spatial resolution of VHR optical satellite imagery necessary for detecting and counting stranded animals, and (3) explore the utility of synthetic aperture radar (SAR) to detect and count stranded animals. We successfully detected and counted large and small stranded odontocetes in optical and SAR satellite imagery. With optical imagery, we found that 0.5 m spatial resolution is suitable for accurately counting large odontocetes (100% accuracy, one image) while 0.3 m resolution is most suitable for counting smaller odontocetes (82–100% accuracy, four images). With SAR, two or more observers detected a total of 108 small odontocetes with high certainty ('likely' or 'definite' detections) compared to 111 in a VHR optical satellite image collected five hours later. These positive results show the potential for stranding networks to expand their monitoring capacity both in terms of scale and speed of detection.

1. Introduction

Effective conservation management of cetaceans requires a deep understanding of local populations and the threats they face (Betty et al., 2020; Jefferson et al., 2011; Stockin et al., 2009). When cetaceans are in distress or unwell, they sometimes wash ashore (alive 'strand' or dead 'beachcast') and are unable to return to the water. Events like this happen due to natural (*e.g.,* age, infectious disease, navigational error, large scale climatic events) or human causes (*e.g.,* bycatch and entanglement, vessel strikes, noise and chemical pollution) and can result in

* Corresponding author at: British Antarctic Survey, High Cross, Madingley Road, Cambridge CB3 0ET, United Kingdom.
E-mail address: clarke.pennyj@gmail.com (P.J. Clarke).

https://doi.org/10.1016/j.ecoinf.2026.103924
Received 18 October 2025; Received in revised form 6 July 2026; Accepted 6 July 2026

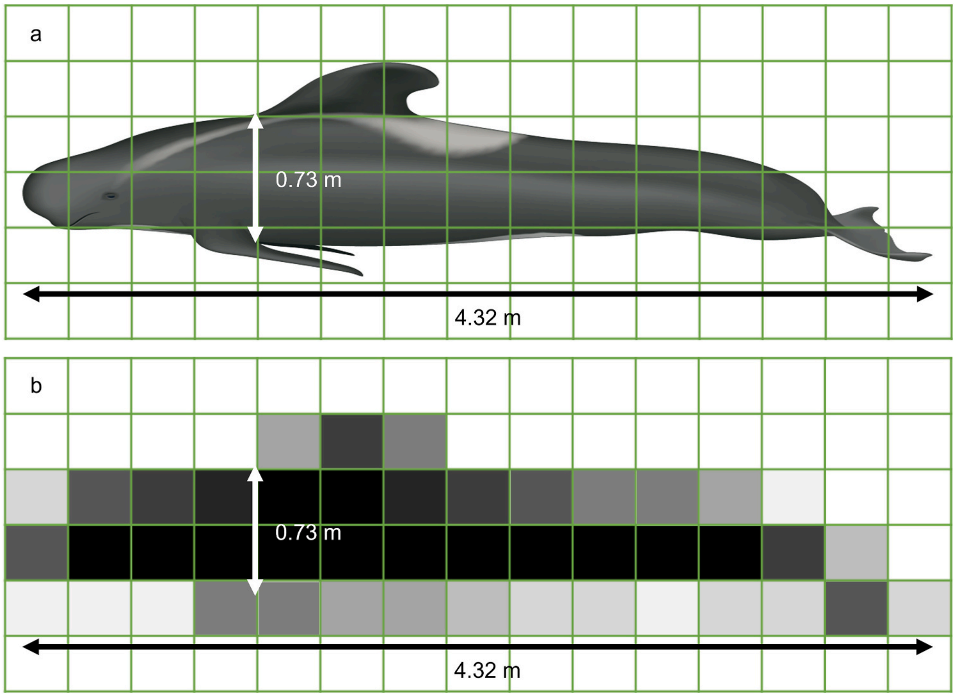

Fig. 1. (a) a long-finned pilot whale (LFPW) illustration (© NOAA) for an average 4.32 m female LFPW (Betty et al., 2022; Betty et al., 2023)), alongside (b) a greyscale representation of the equivalent percentage pixel cover by the LFPW illustration, depicting the expected level of detail visible at the highest commercially available native spatial resolution optical satellite imagery, 0.3 m. Spatial resolution is the distance on the ground represented per pixel.

several animals stranding together (mass stranding (MSE), mass mortality (MME), unusual mortality (UME) events, see Clarke et al., (2021) for definitions). When cetaceans strand, they often act as ocean sentinels, by providing advanced warning to the public of a local environmental threat, anomaly or pollution event (Clarke et al., 2021; Coombs et al., 2019). They provide rare opportunities to examine conditions that affect cetacean populations such as harmful algal blooms, ocean noise, vessel strikes and anthropogenic impacts such as entanglement (Gulland et al., 2025). In addition, data from cetacean strandings can inform our understanding of past and present diversity and distribution of local cetacean populations (Coombs et al., 2019; Roman et al., 2014). Furthermore, reports of cetacean strandings are on the rise, increasing the need for strandings surveillance (Coombs et al., 2019; Leeney et al., 2008; Lennon et al., 2025; Perrin and Geraci, 2009; Pyenson, 2011).

Despite the conservation rationale to study strandings (IWC, 2017), stranding networks globally are infrequent to non-existent in remote, minimally populated, unpopulated and geopolitically unstable regions, and within coastal areas that are complex or have limited economic resources (Clarke et al., 2021). Even in well-resourced regions such as the UK and Ireland, strandings response is often delayed along the complex and sparsely populated coastlines west of Ireland and northern Scotland (Clarke et al., 2025a). Given the importance of strandings for informing cetacean conservation, there is a clear need for new, scalable tools to bridge this monitoring gap.

Very high-resolution (VHR) optical satellites can capture imagery anywhere on Earth, offering the prospect to monitor remote coastal areas at broader spatial and temporal scales than conventional stranding networks. This tool has strong potential to enhance our understanding of stranding patterns to: provide baseline data in remote regions; improve assessments of species' vulnerability to climate change by evaluating changes in stranding rates alongside climate change indicators; and optimise on-the-ground response. VHR optical satellite imagery has already proven useful for detecting and counting stranded large-bodied whale species. For example, stranded sei whales (*Balaenoptera borealis*), were successfully detected and counted from space in the remote Chilean Fjord, Golfo de Penas (Clarke et al., 2021; Fretwell et al., 2019; Häussermann et al., 2017). However, the use of VHR optical satellite imagery is limited by cloud cover, the primary environmental condition governing successful imagery collection (Attard et al., 2025; Clarke et al., 2021; Clarke et al., 2025a; LaRue et al., 2017). Additionally, optical satellites require daylight to capture imagery, prohibiting observations at night and at high latitudes during winter. In contrast, synthetic aperture radar (SAR) satellites enable imaging of Earth in cloudy regions and in darkness (Woodhouse, 2006). SAR satellites have active sensors, which emit radar signals (pulses of microwave radiation) and record the intensity of backscatter reflected from the Earth's surface as brightness values (Woodhouse, 2006). The different biological, chemical, and physical properties of stranded cetaceans, such as their dielectric constant (radiative/absorptive properties of electrical energy, *e.g.,* how radar pulses interact with an animal's lipid-tissues) impact the intensity of backscatter, and could enable their detection from space using SAR (Woodhouse, 2006). Additionally, the rougher a surface, the more intense the reflection and brighter a feature appears (Woodhouse, 2006). Changes in surface roughness caused by a cetacean MSE could also be detectable from space using SAR, similar to dense aggregations of walruses that appear bright relative to smooth or pebbly substrates (Fischbach et al., 2025; Fischbach and Douglas, 2021). As such, it is worth exploring whether cetaceans are similarly bright in SAR imagery. This approach could facilitate strandings detection in cloudy regions, independent of daylight hours, enabling timely emergency responses to unfolding stranding events. The accuracy and limitations of SAR satellites for detecting stranded cetaceans needs to be understood.

Odontocete species (toothed whales and dolphins) comprise the majority of reported MSEs and are mostly much smaller than baleen whales (Aniceto et al., 2021; Clarke et al., 2021; Geraci and Loundsbury, 2005; Hamilton, 2018). With advances in VHR satellite technology and their successful application to study other aggregations of smaller marine wildlife species on shores, such as walruses (*Odobenus rosmarus*; ~1–4 m length) (Cubaynes et al., 2024) and southern elephant seals (*Mirounga leonine*; ~2.4 m length adult female) (Laborie et al., 2023; McMahon et al., 2014), accurate detection and counting of odontocetes should be possible. Pilot whales (*Globicephala spp.*; ~1–6 m length) are a

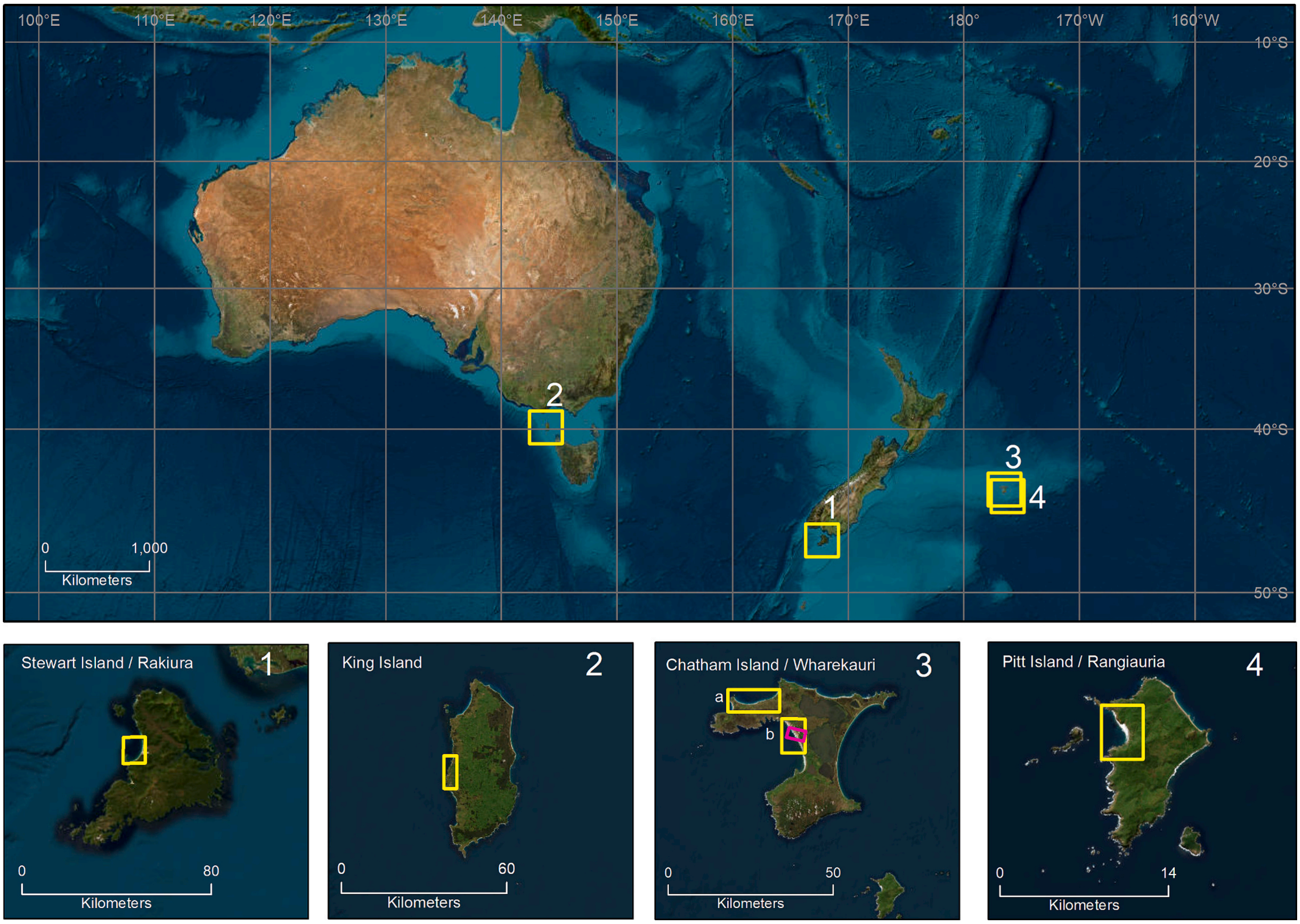

Fig. 2. The five stranding site locations (hollow yellow boxes, main map) and the satellite image extent (hollow yellow box represents optical satellite imagery extent, hollow pink box represents synthetic aperture radar satellite imagery extent, sub-maps 1–4). 3 a and b are comprised of two separate events that occurred on the same island. Service layer credits: source: Esri, Maxar, GeoEye, Earthstar, Geographics, CNES/Airbus, DS, USDA, USGS, AeroGRID, IGN, and the GIS User Community. (For interpretation of the references to colour in this figure legend, the reader is referred to the web version of this article).

species of dolphin commonly known to mass strand (Fig. 1). However, smaller sized animals may also require satellite imagery with higher spatial resolution for their detection, which can increase costs, impacting equitable access and the global integration of this tool to study strandings. There is therefore a need to establish the minimum spatial resolution required to confidently detect and count odontocetes, as well as the types of satellite imagery that can be used (Clarke et al., 2021).

Strandings detection using VHR satellite imagery offers opportunities for monitoring strandings at two scales: detection of an event (to establish baseline data in remote areas where events would otherwise remain undetected), and counting numbers of stranded animals (to achieve more accurate reporting to evaluate changes in stranding rates, and to inform response on the ground). This study aims to; (1) investigate whether small stranded odontocete species can be detected and counted with confidence in VHR optical satellite imagery, (2) determine the minimum resolution of VHR optical satellite imagery required to detect and count small stranded odontocetes with confidence, and (3) explore the use of SAR satellite imagery for detecting and counting stranded odontocetes with confidence. Data from MSEs of long-finned pilot whale (LFPW), on Chatham, Pitt and Stewart Island, New Zealand, and one large odontocete (sperm whale) MSE on King Island, Tasmania, Australia are used to examine these questions in detail.

2. Materials and methods

2.1. Area of study

This study examines five MSEs on remote islands in Tasmania and New Zealand, between 2018 and 2023 (for details of event and study area choice, see supplemental S1). The events comprise: (1) a LFPW mass stranding of 162 individual animals comprising two pods approximately 2 km apart, reported 24 November 2018 in Mason Bay, Stewart Island/Rakiura, New Zealand, (2) a sperm whale mass stranding of 14 individuals, reported 19 September 2022 on King Island, Tasmania, (3a) a LFPW mass stranding of 243 animals, reported 7 October 2022 on Maunganui Beach, Chatham Island/Wharekauri, New Zealand (3b) a LFPW mass stranding of 136 animals, reported 3 October 2023 on Long Beach, Petre Bay, Chatham Island/Wharekauri, New Zealand, and (4) a LFPW mass stranding of 245 animals, reported 10 October 2022 in Waihere Bay, Pitt Island/Rangiauria, New Zealand (Fig. 2).

The four LFPW mass stranding events occurred within similar coastal environments; gentle sloping sandy beaches encapsulated within a protruding section of coast. These coastal topographies are typical of mass stranding sites in the region throughout recorded history (Brabyn and McLean, 1992). The sperm whale mass stranding occurred on an exposed (significant wind, tides and swell/breaking water) section of rocky coast.

2.2. Satellite imagery

Stranding events were selected based on opportunistic availability of satellite imagery within image archives, as well as actively tasking (ordering) new imagery during stranding events. In an archival search of online news and research articles detailing odontocete MSE, MME and UME globally, between 2008 (the launch year of GeoEye-1, the first 0.5 m VHR optical satellite sensor) and 2021, cross-referenced with the Sentinel Hub and Vantor (formerly Maxar Technologies Ltd) archives, we identified two cloud free archival images. The images were a Pleiades image (0.5 m, Sentinel Hub archives (Planet Labs, 2025)) and a WorldView-2 image (0.5 m 'uplifted' to 0.3 m, Vantor archives (Vantor, 2025)). Both were of the LFPW MSEs on Stewart Island (supplemental S2, Table S2.1). For the stranding events in 2022 and 2023, the team worked with the Department of Natural Resources, Tasmania and the Department of Conservation, New Zealand to coordinate image tasking in real time as the event unfolded. This resulted in a further seven images (supplemental S2). Imagery can be acquired from satellite image providers at differing levels of pre-processing, the data analysed here was acquired to include a UTM map projection (see supplemental S2 and Clarke et al., (2026a)), to achieve a more accurate flat two-dimensional representation of the Earth.

To establish the minimum spatial resolution required for confident detection and counting of odontocete strandings, optical satellite images were collected at their sensor specific native spatial resolution (0.5 or 0.3 m) and were artificially down-sampled (reduced spatial resolution), and/or up-sampled (enhanced spatial resolution) by the satellite image provider, to achieve, where possible, imagery at three spatial resolutions, 0.5, 0.3 and 0.15 m (supplemental S2). Vantor's proprietary 'High-Definition (HD) technology' applies a complex fine-tuned mathematical model to increase the number of pixels, to achieve an 'uplifted' spatial resolution product (Vantor, 2020). The availability to down-sample or up-sample an image was dependent upon the native spatial resolution of the product. For example, native 0.5 m spatial resolution imagery can be up-sampled to 0.3 m, and native 0.3 m spatial resolution imagery can be down-sampled to 0.5 m or up-sampled to 0.15 m.

A SAR image provided by Airbus through Deutsches Zentrum für Luft- und Raumfahrt's (DLR) TerraSAR-X sensor in Staring Spotlight mode, with an azimuth resolution of 0.51 m and a ground range resolution of 1.27 m, resulting in a 0.28 m spatial resolution (projected spacing azimuth, 5 by 5 km scene), was acquired to assess SAR's utility for detecting and counting stranded cetaceans (see DLR's basic product manual, Section 2.1.2.3 (Eineder et al., 2013)). The SAR image was collected concurrently (five hours later) with a matched optical collection from Vantor's WorldView-3 sensor. Details of all imagery used in this analysis, including metadata and information necessary to access and reproduce the image pre-processing steps, are provided in supplemental S2 and in Clarke et al., (2026a).

2.3. Direct counts

Direct counts used in this study include ground counts or counts made in aerial imagery. In all instances, ground counts available were total counts (number of animals) that we used to compare with satellite counts (Cubaynes et al., 2024). For the sperm whale event in Tasmania, ground counts collected by a local stranding network were provided by the Department of Natural Resources and Environment, Tasmania. Ground counts were collected one day after the event was reported (20 September 2022) and eight days prior to satellite image collection (28 September 2022). These data included positional information (latitude and longitude) for all but one individual.

For all LFPW events, ground counts collected by local stranding networks were provided by the New Zealand Department of Conservation, except for Pitt Island, where total counts were acquired from reports communicated online at the time of the event unfolding by the New Zealand strandings Non-Governmental Organisation, Project Jonah. Aerial imagery was available for the Stewart and Chatham Island (3a) events, collected and provided by the Department of Conservation and a local photographer, respectively, capturing part of the event extent. Aerial imagery was annotated as detailed in Section 2.4, to achieve a total count for comparison with satellite counts.

2.4. Image pre-processing and manual annotation

We used Clarke et al., (2026a) open-source QGIS (version 3.28) workflow to pre-process and annotate satellite imagery. All VHR optical satellite imagery were pansharpened using a QGIS plugin, Orfeo Toolbox (version 8.1.1. Win64, BundleToPerfectSensor tool, Bayes algorithm and bi-cubic interpolation, see supplemental S2), to produce a multispectral image with the higher spatial resolution of the panchromatic image. Orfeo Toolbox was selected over GDAL for pansharpening, for its ability to preserve all spectral bands in processing. A challenge to annotating satellite imagery is inter observer variation in counts, which varies depending on image spatial resolution and quality (Cubaynes et al., 2024). Therefore, we used three observers with a high level of expertise in reviewing satellite imagery for wildlife from space, to independently review the satellite imagery using the annotation workflow to assess confidence in the annotations. Observers had the following target feature expertise; observer 1 - live and stranded whales, observer 2 - live whales and walruses, and observer 3 - albatrosses and walruses. Additionally, observers 1 and 2 had field experience (ground and aerial surveys) observing live and stranded cetaceans. For each stranding event, they reviewed imagery sequentially from low to high spatial resolution to avoid introducing biases when reviewing lower resolution satellite imagery. For accurate comparison between observers, all annotations were made in true colour (red, green, blue bands) under the same band rendering properties, *e.g.,* contrast enhancement, brightness, contrast, saturation and gamma. Observers were provided training for how to score features of interest in the imagery. Features were recorded with a georeferenced point and assigned a confidence score, definite (90–100%), likely (70–89%) and possible (50–69%). For example, visible whale-defining features (*e.g.,* fluke, flippers) would help an observer assert definite (90–100%) certainty to a detection. For details of how scores are derived, see supplemental S3 of Clarke et al., (2026a) and Cubaynes et al., (2023). Additionally, observer 1 annotated all features with the required and desirable attributes outlined in the standardised protocols developed by Clarke et al., (2026a). As a final stage, observers annotated aerial imagery using the Visual Geometry Group Image Annotator, following protocols in Cubaynes et al., (2024).

For SAR image counts, the SAR image was georeferenced to the matching optical image (aligning both images by assigning six ground control points (GCP) in the SAR image to known geolocations in the optical image, using the 'Georeferencer' tool in QGIS 3.16, transformation type: polynomial 1 and resampling method: linear, see supplemental S3 and S4). The SAR and optical images were split in half, and the opposite halves of the corresponding imagery were provided to each observer in two separate experiments. This ensured the observer SAR counts were independent of visual aids from the optical imagery, while still allowing coastline alignment for reference. Annotations were marked using the same procedure as for optical imagery, except observer 1 assigned only required attributes, due to a lack of visual cues for annotating each point with desirable attributes.

2.5. Semi-automated clustering of multi-observer annotations

To compare observers' annotations, hierarchical clustering was performed using a python script (v3.12) adapted from Attard et al., (2025) (available at: doi:https://doi.org/10.5281/zenodo.20547057; Clarke et al., 2026b), with the most up-to-date version found at: https://github.com/PennyJClarke/strandings_from_space). The semi-automated (automated clustering requiring manual validation of performance)

Table 1
Observer counts (observer 1: blue, observer 2: orange, and observer 3: green) by certainty of a stranded cetacean detection (definite, likely, possible), per (optical and synthetic aperture radar) satellite image catalogue ID and spatial resolution, and aerial image, compared to ground counts, and performance of semi-automated clustering of multi-observer annotations. Plot references and observer colour correspond with Fig. 3.

Species	Plot	Location/Image Cat ID/Image Date YYYY-MM-DD (UTC)/Ground count date (days before (+)/after (-) satellite image)	Sensor type	Spatial resolution (m)	Ground/Reference count	Definite	Likely	Possible	Certainty agreement[1]	Cluster # 3	Cluster # 2	Cluster # 1	Ground count agreement (%)[1]	Observer agreement (%)[1]	Rand index (Adjusted Rand index)
Sperm whale (*Physeter macrocephalus*)	A	Location: King Island Image cat ID: 105001002F0CA400 Image date: 2022-09-28 Ground count date: 2022-09-20 (+8)	GeoEye-1 (Optical)	0.5	14	14	0	0	1	13	1	0	100		1 (1)
						14	0	0							
						8	5	0							
				0.3		14	0	0	1	14	0	0	100		1 (1)
						14	0	0							
						14	0	0							
Pilot whale (*Globicephala* spp.)	B	Location: Long Beach, Petre Bay, Chatham Island (3b) Image cat ID: C542_N85_D_ST_spot_029_R_ 2023-10-05T17:04:56.332868Z[2] Image date: 2023-10-05	TerraSAR-X (SAR)	0.28	NA	0	102	64	NA	75 (58)	59 (50)	77 (67)	NA	63.51	1 (0.99)
						1	85	81							
						0	87	0							
	C	Location: Long Beach, Petre Bay, Chatham Island (3b) Image cat ID: 104001008D07E000[2] Image date: 2023-10-05 Ground count date: 2023-10-03 (+2)	WorldView-3 (Optical)	0.3	136	102	25	99	0.93	109 (79)	67 (32)	87 (30)	129.41		1 (0.99)
						121	16	76							
						10	60	39							
	D	Location: Maunganui Beach, Chatham Island (3a) Image ID: 105001002F60AA00 Image date: 2022-10-14 Ground count date: 2022-10-08 (+6)	GeoEye-1 (Optical)	0.5	243	148	72	41	0.69	133	48	82	74.49		1 (0.93)
						167	0	15							
						5	50	79							
	E	Location: Maunganui Beach, Chatham Island (3a) Image ID: 10300100DC306300	WorldView-2 (Optical)	0.5	243	160	50	35	0.86	130	90	103	90.53		1 (0.95)
						187	25	84							
						0	51	81							

	Image date: 2022-10-19		0.3		118	70	44	0.69	151	49	48	82.30		1
	Ground count date: 2022-10-08 (+11)				144	24	41							(0.97)
					24	75	58							
F	Location: Maunganui Beach, Chatham Island	WorldView-3	0.5	243	181	36	27	0.84	161	49	41	86.42		1
	(3a)	(Optical)			198	5	12							(0.96)
	Image ID: 104001007E5E7400				3	84	76							
	Image date: 2022-11-03		0.3		174	48	34	0.91	192	36	40	93.83		1
	Ground count date: 2022-10-08 (+25)				209	11	6							(0.99)
					0	146	60							
			0.15		151	75	52	0.92	218	31	41	102.47		1
					206	17	20							(0.98)
					103	89	44							
G	Location: Pitt Island/Rangiauria	WorldView-2	0.5	245	44	110	65	0.63	79	82	65	65.71		1
	Image ID: 10300100DB012A00	(Optical)			152	9	5							(0.96)
	Image date: 2022-10-21				0	18	65							
	Ground count date: 2022-10-10 (+11)													
H	Location: Stewart Island/Rakiura	Pleiades	0.5	162	79	16	7	0.59	84	15	9	61.11		1
	Image ID: DS_PHR1B_201811282258003	(Optical)												(0.99)
	_FR1_PX_E167S47_1106_03071				98	1	4							
	Image date: 2018-11-28				34	36	16							
	Ground count date: 2018-11-24 (+4)													
I	Location: Stewart Island/Rakiura	WorldView-2	0.5	162	92	30	24	0.75	91	43	15	82.72		1
	Image ID: 1030010089B22D00	(Optical)			127	7	2							(0.95)
	Image date: 2018-12-02				13	31	48							
	Ground count date: 2018-11-24 (+11)		0.3		110	33	28	0.86	113	36	30	91.98		1
					132	8	15							(0.98)
					42	52	21							
	Location: Maunganui Beach, Chatham Island	Aerial	0.05[3]	NA	120	0	0	NA	119	2	2	NA	98.37	1
	Image date: 2018-10-08				121	0	2							(1)
	Source: Tamzin Henderson				119	0	1							
	Location: Stewart Island	Aerial	0.02[4]	NA	116	2	3	NA	120	1	3	NA	97.58	1
	Image date: 2018-11-24				124	0	0							(1)
	Source: Department of Conservation				113	6	1							

[1]Median certainty agreement = median(definite + likely / reference), Ground count agreement = (Cluster #3 + Cluster #2)/reference, Observer Agreement = (1 – (Cluster #1 / (Cluster #3 + Cluster #2)) *100).
[2]Within the cluster # columns, the values in brackets for image catalogue ID 3490335 and 104001008D07E000, are the cluster totals in the shared cloud-free regions of the matched optical and SAR images.
[3]Estimated spatial resolution based on image calibration using average whale length (4.91 m) = 1 / 42.4901 pixels m-1.
[4]Estimated spatial resolution based on image calibration using average whale length (4.91 m) = 1 / 17.6850 pixels m-1.

approach to clustering used Wards method to amass point annotations of a stranded animal by multiple observers, to efficiently evaluate count congruence between observers. See supplemental S5 for more details. To assess the accuracy of automated clustering, we calculated a Rand index (RI) and adjusted Rand index (ARI) for each image.

2.6. Count accuracy

We considered the agreement between observers in aerial imagery for LFPW, and observer agreement with the ground count in the sperm whale satellite imagery, as a baseline for evaluating our confidence in comparisons between observers within the LFPW satellite imagery analysis. We made this assumption given that satellite imagery has already proved to contain identifiable, and countable, baleen whales, which are a similar size to sperm whales (13–15 m) (Corrêa et al., 2022; Cubaynes et al., 2019; Fretwell et al., 2014; Fretwell et al., 2019), and the associated aerial imagery of pilot whales is highly detailed. Thus, it is expected that observer counts would be accurate within these imagery, and that agreement between observers would be high.

To test the impact of spatial resolution on count accuracy, we eval-

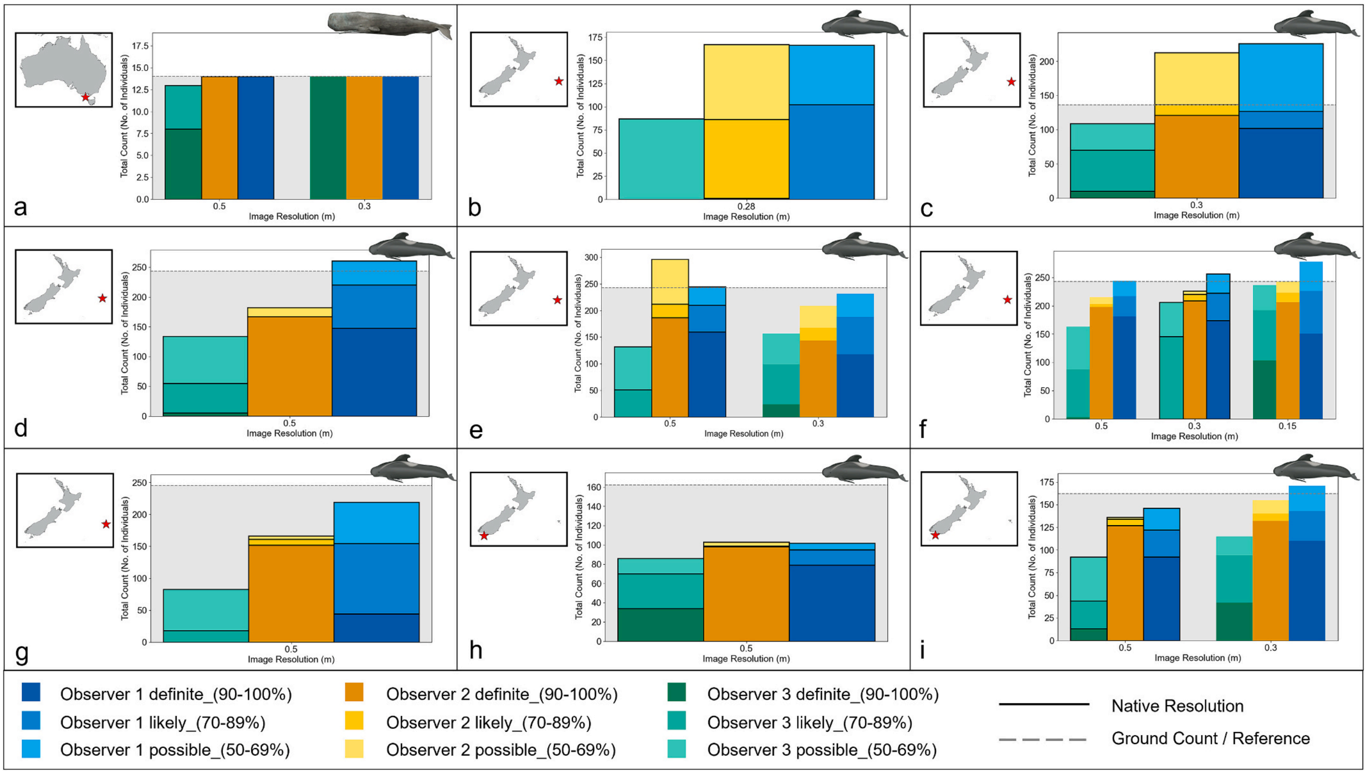

Fig. 3. Stacked bar plots showing the number of carcasses counted by observers (y-axis) at different levels of detection certainty (represented by bar colour) across various image resolutions (x-axis) for each satellite image. Native spatial resolution imagery is represented by a solid black outline on the corresponding spatial resolution barplot. Images were collected opportunistically close in time to *in situ* carcass counts (represented by a dashed horizontal line). Images are identified a-f and cross-referenced in Table 1. Plot B of the synthetic aperture radar image does not include a reference line, as the image extent was smaller than the stranding event and not comparable. The location of the stranding event is detailed by a red star on the location map inset per plot, along with an illustration of a cetacean denoting the stranded species (sperm whale and long-finned pilot whale illustration insert: © NOAA). (For interpretation of the references to colour in this figure legend, the reader is referred to the web version of this article).

uated variation in observer agreement using two metrics, (1) median certainty agreement $= median\left(\frac{(definite+likely)}{reference}\right)$: where the median of features assigned as 'definite' or 'likely' by observers was compared to the ground count, and (2) agreement with the ground count $= \left(\frac{(cluster\#3+cluster\#2)}{reference}\right)*100$: comparing clusters where two or more observers identified a feature when compared to the ground count. Cluster #x notation indicates the number of observers that labelled an object, *e.g.,* cluster #2 refers to clusters where two people labelled an object, and cluster #3 when three people labelled an object. Assessment of observer agreement included detections at all levels of certainty, including possible detections, recognising that individual observers may identify possible detections differently.

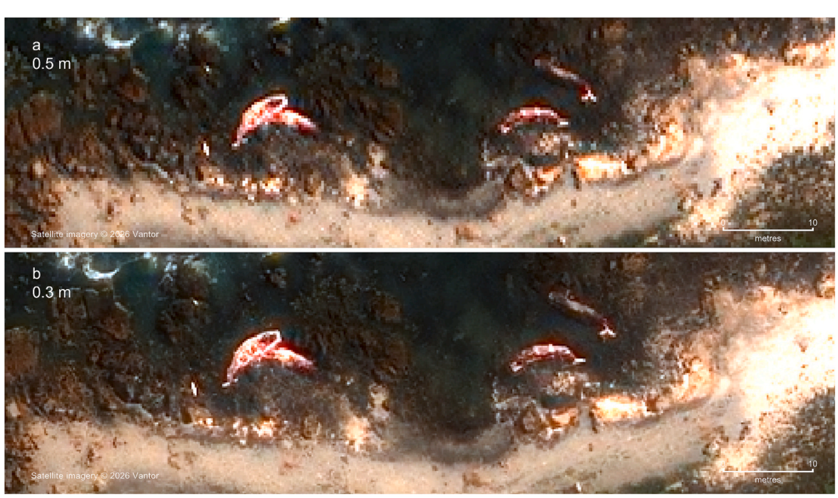

Fig. 4. VHR optical satellite image collected 28 September 2022 by GeoEYE-1, of the King Island sperm whale mass stranding. The imagery demonstrates the high level of detail available for confident detection of sperm whales at (a) 0.5 m and (b) 0.3 m spatial resolution satellite imagery, due to size, visible cetacean-like features (ellipsoid shape and visible fluke) and distinct colour compared with their surrounding environment.

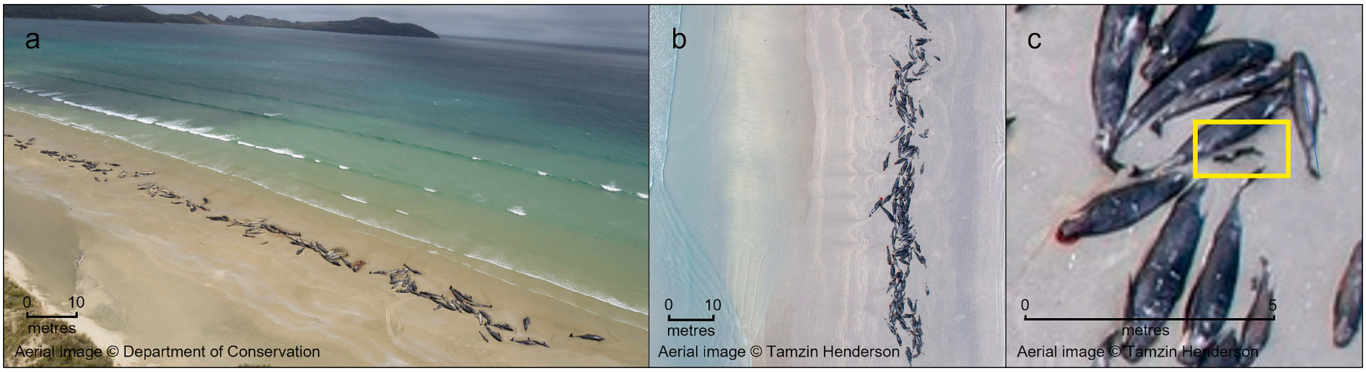

Fig. 5. Aerial imagery counted by observers, (a) of the Stewart Island long-finned pilot whale (LFPW) mass stranding, 24 November 2018, and (b) the Chatham Island LFPW mass stranding event 8 October 2022. (c) Example of erroneous detections made by non-stranding experts in aerial imagery, where buried tailstocks separating the fluke from the main carcass body give the appearance of an individual carcass, which due to size could be misidentified as a calf.

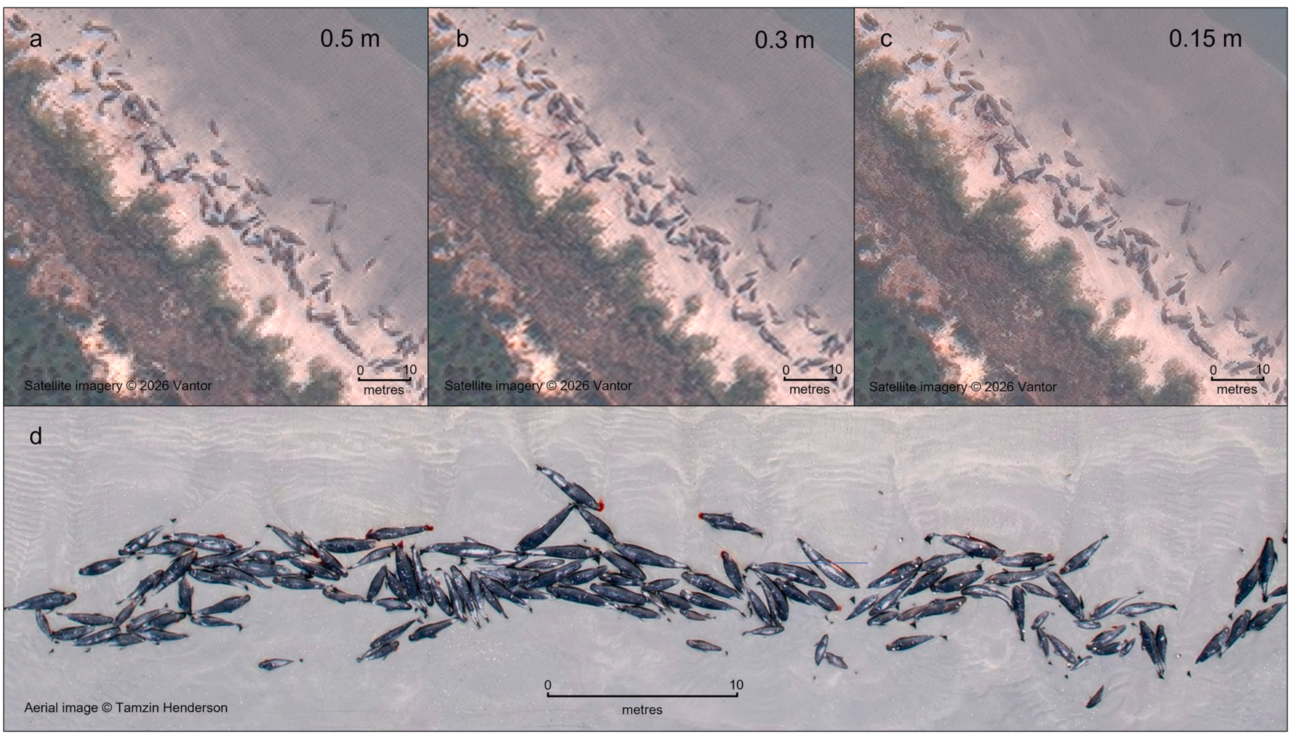

Fig. 6. VHR optical satellite image collected on 3 November 2022 by WorldView-3, of the Chatham Island long-finned pilot whale mass stranding reported on the 8 October 2022, showing three spatial resolutions: (a) 0.5 m downsampled spatial resolution, (b) native 0.3 m spatial resolution captured by the satellite sensor, and (c) 0.15 m uplifted spatial resolution, alongside (d) an aerial image capturing part of the event extent collected on the 8 October 2022.

For the SAR and aerial imagery, the image footprint did not cover the full spatial extent of the event. Therefore, comparison to the ground count could not be made, and agreement between observer counts was calculated using the formula: Agreement between observers = $\left(1-\left(\frac{c}{(a+b+c)}\right)\right)$*100, where a = clusters of three points (all observers agree), b = clusters of two points, and c = clusters of one point (only one observer identified the point).

3. Results

In total, there were 28 sperm whale and 2,568 LFPW detections in VHR optical imagery (across different spatial resolutions, 0.5, 0.3, and 0.15 m), 211 LFPW detections in SAR imagery, and 247 LFPW detections in aerial imagery (inclusive of possible detections, see Table 1 and the open-access dataset available at: https://doi.org/10.5285/b26c3a3d-73c8-4500-9a23-696011c20a45 (Clarke et al., 2025b)).

3.1. Clustering accuracy

Semi-automated clustering enhanced the efficiency of evaluating count congruence. In the case of the baseline imagery, both the aerial imagery of LFPW and optical satellite imagery of sperm whales clustered with 100% accuracy (Table 1). For the VHR satellite imagery of LFPW, a few manual corrections to the clusters were required, however, in the evaluation of performance, the RI in all cases was >0.99, and the more robust measure of performance, ARI, achieved >0.93 (Table 1).

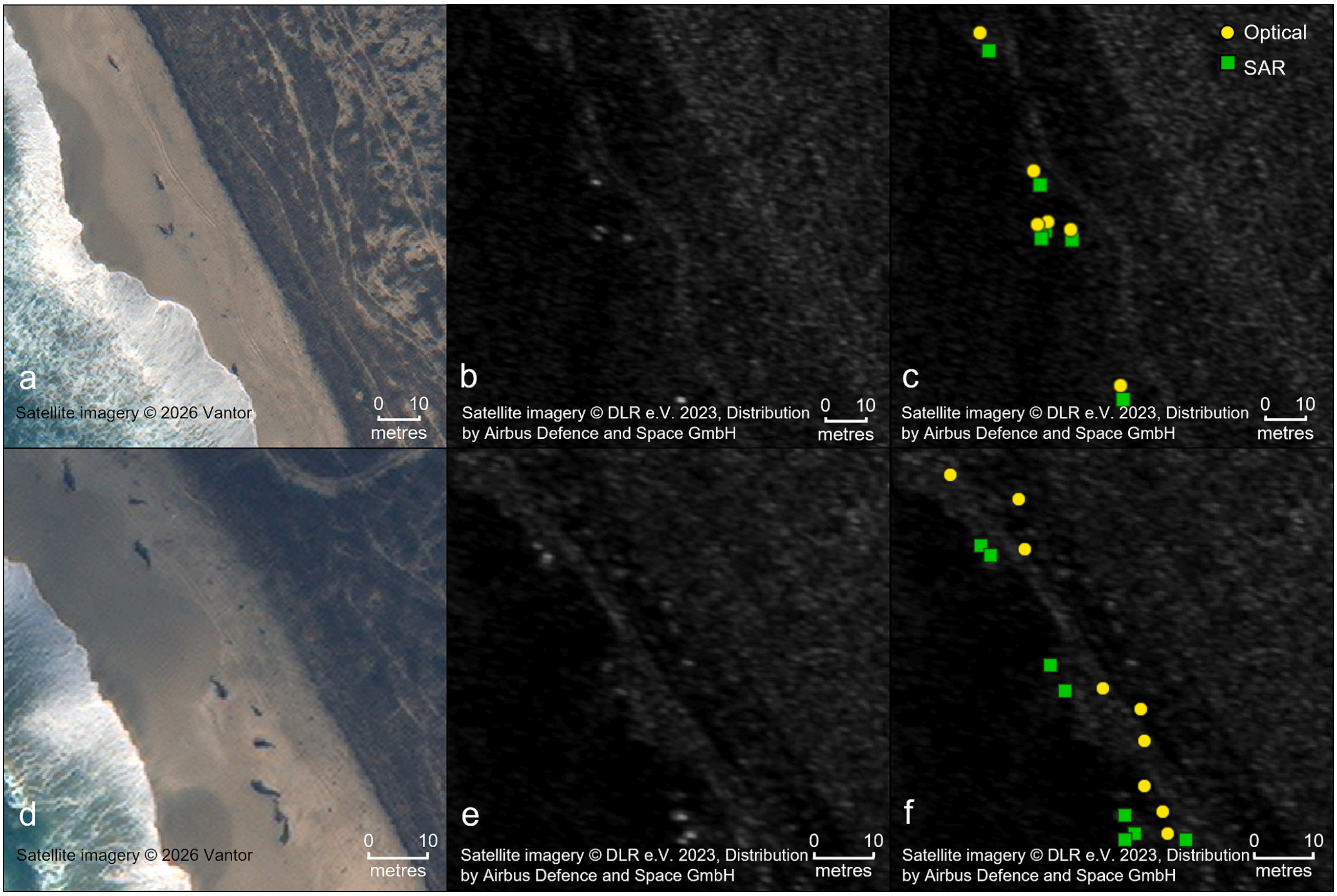

Fig. 7. Examples of long-finned pilot whale in very high-resolution 0.3 m optical satellite imagery (a and d), alongside matched 0.28 m synthetic aperture radar (SAR) imagery (b and e). Clustered observer annotations from optical (yellow circle) and SAR (green square) imagery are overlaid on the SAR image (c and f). (For interpretation of the references to colour in this figure legend, the reader is referred to the web version of this article).

3.2. Count accuracy

3.2.1. Baseline data to evaluate observer agreement

When identifying stranded sperm whales, observers had high agreement with the ground count, achieving 100% accuracy at both 0.5 and 0.3 m spatial resolution for VHR optical satellite imagery (Fig. 3a, Fig. 4, Table 1). Observers also achieved strong agreement, >97%, between two and three observer counts of LFPW in aerial imagery (Table 1, Fig. 5).

3.2.2. LFPW counts in VHR optical satellite imagery

There was substantial variability in observer agreement with the ground count and median certainty agreement across the seven LFPW satellite images examined. In the best case (the Chatham Island LFPW mass stranding, 3 November 2022), confident LFPW detection could be made at all resolutions, 0.5, 0.3 and 0.15 m (Fig. 6). There was high observer agreement with the ground count (>86%), which increased with spatial resolution. When reviewing only the proportion of detections where observers were confident in their observations (definite or likely features), the median certainty agreement between observers was high (>84%) and increased with spatial resolution. Observer certainty increased 7% between 0.5 and 0.3 m spatial resolution; increasing spatial resolution upward to 0.15 m resulted in negligible gain (1%) (Table 1). Furthermore, observers 1 and 2 identified fewer definite and more possible detections at 0.15 m, compared to 0.3 m.

Lowest agreement with the ground count was 61%, and the lowest median certainty agreement was 59%, both recorded for the Pleiades image of the Stewart Island mass stranding (Fig. 3h, Table 1). The WorldView-2 image of the Pitt Island mass stranding yielded similar results; observers achieved a 65% agreement with the ground count and a 63% median certainty agreement (Fig. 3g, Table 1). In some instances, observers overestimated the event size, such as the image captured of the Chatham Island stranding on 5 October 2023, where two or more observers ($n = 176$) exceeded the ground count ($n = 136$) by 29% (Fig. 3c, Table 1).

3.2.3. LFPW counts in SAR satellite imagery

Reviewing only observer counts in the shared cloud free regions between the SAR and matched optical satellite image, where two or more observers identified the same feature, the cluster counts were very similar at 108 and 111 individual carcasses, respectively (Table 1). Direct comparison between optical and SAR imagery could not be achieved to verify if these totals corresponded to the same individuals, due to a five-hour time difference between SAR and optical acquisitions (carcasses may have moved onshore or offshore in the intervening time; Fig. 7c and f). Despite georeferencing the SAR image, there was a small geographical shift between known landmarks and the points in the two images, which could not be rectified with a uniform transformation (*e.g.*, shifting points by a set distance). The georeferencing errors arose due to a limited number of available distinct static features in the matched optical and SAR imagery to define GCPs, and a spatial bias in assigned GCPs resulting from cloud cover obscuring parts of the matched optical image. As such, the presence of confounding features, low-certainty detections, and georeferencing discrepancies further complicated direct feature matching. Fig. 7a, b, and c illustrate cases where detections in optical and SAR can be easily matched, while d, e and f

Fig. 8. Example satellite imagery to visualise causes of low agreement of observer counts with the ground count and median certainty agreement. (a) a 0.3 m spatial resolution optical satellite image collected 5 October 2023 by WorldView-3, of the Chatham Island long-finned pilot whale (LFPW) mass stranding event, showing frequent organic beach debris confounding detection of stranded cetaceans, (b) a 0.5 m spatial resolution optical satellite image collected 21 October 2022 by WorldView-2, of the Pitt Island LFPW mass stranding event, showing a dark sandy beach and resulting low contrast of stranded LFPW with their environment, and (c) a 0.5 m spatial resolution optical satellite image collected 14 October 2022 by GeoEYE-1, of the Chatham Island LFPW mass stranding event, showing the challenge of detecting individual stranded cetaceans in hazy thin cloud.

highlight challenges in matching detections due to the five-hour time difference between SAR and optical acquisitions and a georeferencing discrepancy. Analysis of agreement between observers in SAR revealed low congruence at only 64% agreement (Table 1). The low agreement can be attributed to the high numbers of detections in SAR made by a single observer (the portion of disagreements), of which 87% were lower certainty (possible) detections.

4. Discussion

Here, we describe the first detection and count of odontocete strandings in both VHR optical and SAR satellite imagery.

4.1. VHR optical satellite imagery: detection and count

When observers reviewed images with sufficient resolution to show whale-defining features, observers achieved high agreement in detecting small odontocete species in aerial imagery, and large odontocetes in VHR optical satellite imagery. The few errors in detections in aerial imagery occurred when non-stranding experts misidentified LFPW flukes as possible calves, due to buried tail stocks (Fig. 5c), and in VHR optical satellite imagery, a stranded sperm whale was missed when obscured by cloud shadows on a low contrasting rocky shore. As a baseline comparison, the aerial imagery of LFPW and optical satellite imagery of the sperm whale showed that observer counts were very similar to one another, demonstrating that observers are capable of accurate annotations when the feature is clearly visible.

Our study shows that LFPW can be detected and counted with confidence in VHR optical satellite imagery. The VHR optical satellite image with best observer agreement with the ground count, and high median certainty agreement across all three spatial resolutions (image cat id 104001007E5E7400, Table 1 Fig. 3f, Fig. 6), can be attributed to the ideal conditions of the image collection. The stranding location was cloud-free, the environment was highly contrasting (dark LFPW on a light sandy beach), and there were few to no confounding features, such as organic beach debris. Despite the high-count accuracy achieved for this image, agreement was still lower than for the sperm whale, which is intuitive given their size difference. Aside from their smaller size and often absence of whale-defining features visible in VHR optical satellite imagery, the density of LFPW carcasses compared to the sperm whale (large numbers of individuals in close proximity, often touching or overlapping) is likely to make individual detections more challenging and reduce count accuracy. Greater variability in counts between observers for species that aggregate in large numbers has been reported in other remotely sensed animal monitoring studies (Attard et al., 2024; Bird et al., 2020).

For LFPW strandings, we found lower observer agreement with the ground count and lower median certainty agreement when image quality was poor and/or when the environment had a lot of confounding features or low contrast to the stranded animals. This finding aligns with other wildlife from space studies (Charry et al., 2021; Fretwell et al., 2017; LaRue et al., 2011; Stapleton et al., 2014). Observer experience was also an interplaying factor influencing level of agreement when image quality or environmental conditions were suboptimal. The lowest agreement compared with the ground count (61%), and lowest median certainty agreement (59%), occurred in the first image reviewed by all observers (Pleiades image of the Stewart Island mass stranding, Table 1), suggesting observer training and expertise in remote sensing and of the target feature is important. However, the >90% similarity between different observer counts for this image (Fig. 3h) suggests the low overall agreement with the ground count was due to other factors like low spatial resolution and a high incidence angle (off-nadir) of the image collection. The spatial resolution of the final processed image delivered by the satellite image provider was 0.5 m, however, the raw spatial resolution of the collection was ~0.81 m. This image had the coarsest raw spatial resolution and largest difference in resampling spacing (difference between the raw and product spatial resolution) of all VHR optical satellite imagery. Additionally, a higher off-nadir angle (24.2°) reduces the spatial resolution and clarity, and therefore interpretability, of an image. While it is possible that some carcasses washed offshore, reducing the number compared to the ground count, a later optical satellite image collected four days after the event showed >82% observer agreement with the ground count (Fig. 3i, Table 1).

All observers had wildlife remote sensing expertise, but observer 3 had less experience with the target species and stranding events. This may have led to their lower detection certainty in all imagery compared to observers 1 and 2, however, it is challenging to disentangle whether this observer applied caution in their detections/certainty,

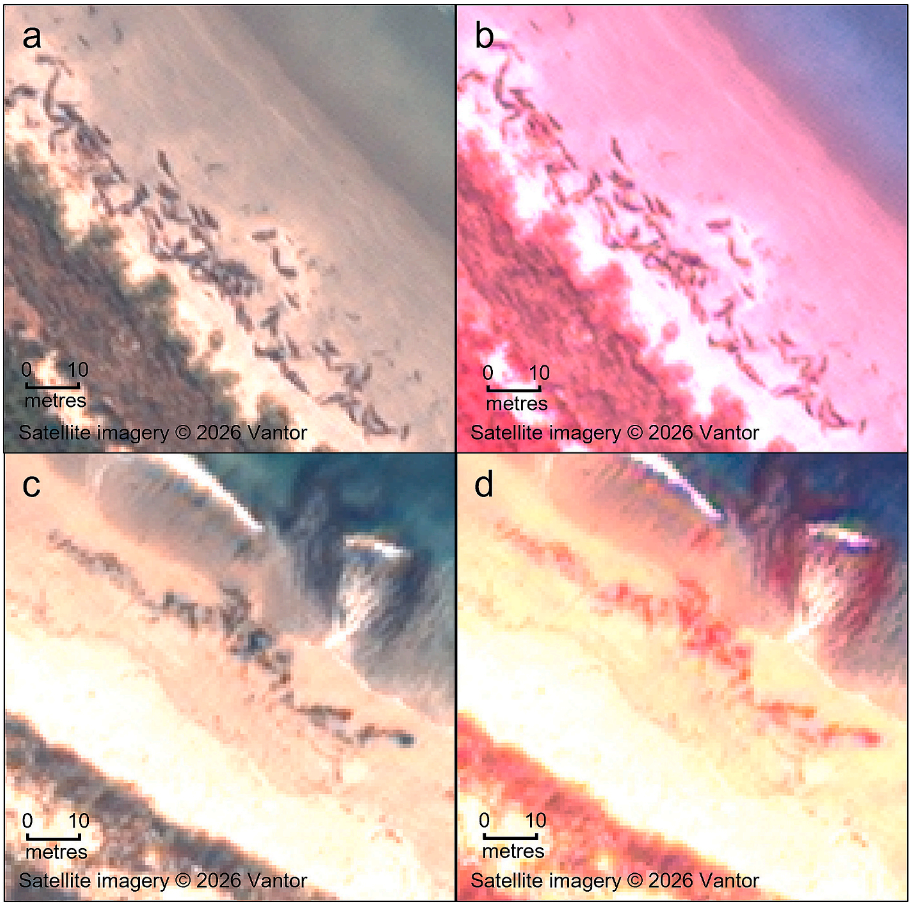

Fig. 9. 0.5 m eight band optical satellite image collected 19 October 2022 by WorldView-2, of the Chatham Island long-finned pilot (LFPW) whale mass stranding event, demonstrating the power of band combination manipulation to differentiate stranded cetacean carcasses from confounding features, such as organic beach debris, in satellite imagery. (a) Band combination R = red (5), G = green (3), B = blue (2), showing stranded LFPW carcasses, (b) the same image as (a), only this time displayed in band combination R = red edge (6), G = yellow (4), B = green (3). Using this band combination vegetation appears red and stranded cetacean carcasses remain as spectrally unique dark bodies. (c) Band combination R = red (5), G = green (3), B = blue (2), showing organic beach debris, (d) the same image as (c), only this time displayed in band combination R = red edge (6), G = yellow (4), B = green (3). Using this band combination vegetation appears red, including organic beach debris such as algae, allowing differentiation from stranded cetacean carcasses. RGB here refers to the QGIS display settings, while the band name and number refers to the specific band of the WorldView-2 multispectral sensor. (For interpretation of the references to colour in this figure legend, the reader is referred to the web version of this article).

acknowledging their own limitations. To minimise observer variation, Attard et al., (2024) emphasised the importance of observer training and expertise with the target species, as well as implementation of standardised workflows, and our results support these recommendations.

Features like algae confound the detection of LFPW carcasses due to their similar colour and shape, resulting in non-cetacean features being misidentified as stranded cetaceans, inflating counts and agreement with the ground count. For example, in the 5 October 2023 optical satellite image of the Chatham Islands stranding, the 129% agreement with the ground count, indicating overcounting, could be attributed to the presence of extensive organic beach debris (Fig. 8a). The human eye sees only in the visible range of the electromagnetic spectrum; however, satellites capture information beyond the visible range, which could help distinguish carcasses from confounding features (Attard et al., 2024; Fretwell et al., 2019; Rees, 2013). In the red edge and near infrared (NIR) bands, vegetation appears red, whereas carcasses remain spectrally unique (Fig. 9b and d). This supports previous applications of satellites to study strandings, where Fretwell et al., (2019) developed this methodology to document that sei whale carcasses exhibited a high reflectance in NIR, allowing discrimination from confounding features such as logs. NIR, when available, could help eliminate confounding features to achieve more accurate and confident detections (Clarke et al., 2021). Despite over-estimating the size of the event, the median certainty agreement between observers in this image (104001008D07E000, 93%, Table 1) was the highest achieved in all LFPW satellite imagery. This likely resulted from the low density of carcasses spread across a large area, making individual carcasses easier to identify, as seen for sperm whales which also tend to be more scattered.

Low contrast between the target feature and the surrounding environment, along with cloud cover, both reduced the detection accuracy and counts of LFPW. This has been similarly documented in previous studies using VHR optical satellites to study wildlife (Abileah, 2002; Attard et al., 2025; Bamford et al., 2020; Boulent et al., 2023; Charry et al., 2021; Clarke et al., 2021; Cubaynes et al., 2019; Fretwell et al., 2014; Fretwell et al., 2019; Höschle et al., 2021; Khan et al., 2023; LaRue et al., 2017; Lennert-Cody et al., 2019; Platonov et al., 2013). For example, the second-lowest agreement with the ground count and median certainty agreement occurred in the WorldView-2 image of the Pitt Island mass stranding, where low contrast between the LFPW carcasses and the dark sandy beach (Fig. 8b, Table 1), and high off-nadir angle (28.1°), reduced detection accuracy. The third-lowest agreement with the ground count and median certainty agreement coincided with cloudy conditions in the 14 October 2022 GeoEYE-1 image of the Chatham Island LFPW stranding. We observed that even the thinnest of

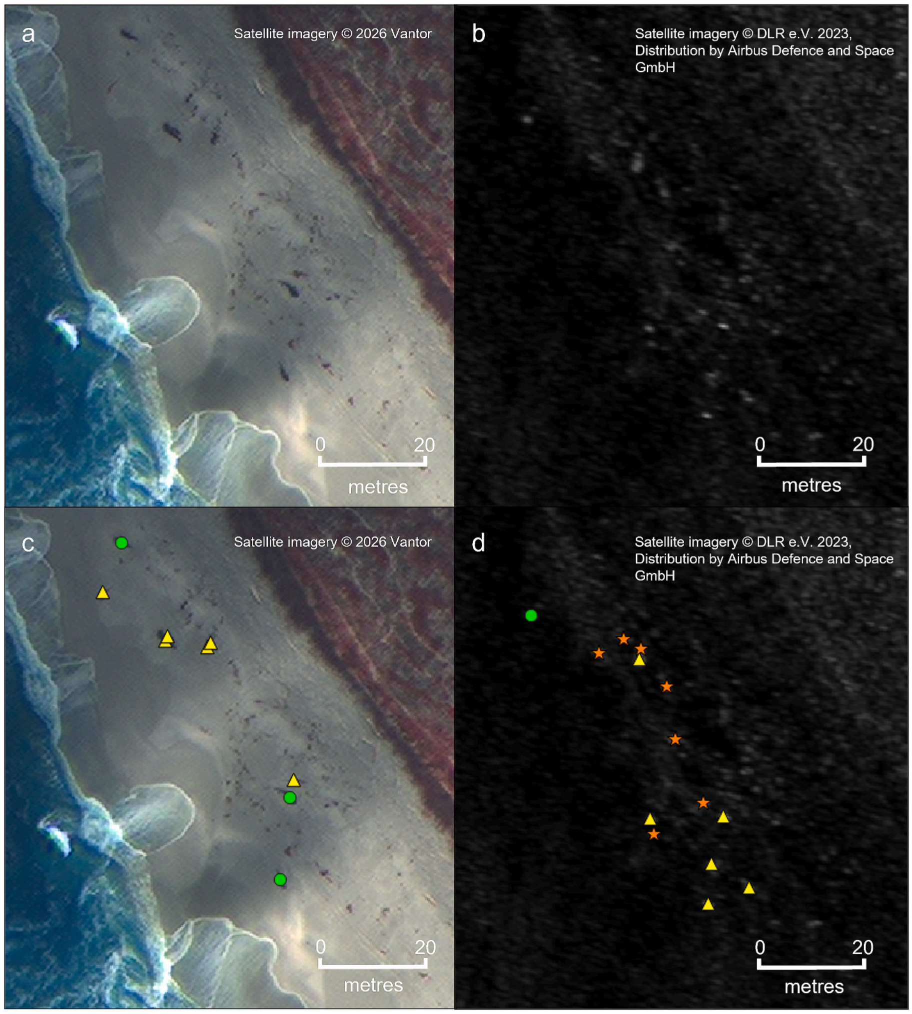

Fig. 10. (a) and (c) a 0.3 m spatial resolution VHR optical satellite image collected 5 October 2023 by WorldView-3, displayed in band combination R = red edge (6), G = yellow (4), B = green (3). Using this band combination vegetation appears red and stranded cetacean carcasses remain as spectrally unique dark bodies. RGB here refers to the QGIS display settings, while the band name and number refers to the specific band of the WorldView-3 multispectral sensor. (b) and (d) a matched (concurrent within five hours) 0.28 m spatial resolution synthetic aperture radar (SAR) image. Green circles represent stranded cetacean features identified by three observers, yellow triangles by two observers, and orange stars by one observer. (For interpretation of the references to colour in this figure legend, the reader is referred to the web version of this article).

cloud cover reduced detection accuracy and certainty (Fig. 8c, Table 1).

Our study has a few methodological limitations, which are hard to overcome when ground-truthing satellite imagery. These include the timing of satellite image collections so that they are captured straight after a stranding occurs, and are coordinated with the ground counts and aerial imagery. Timing was governed by cloud cover, satellite revisit rate, and costs of priority tasking (see supplemental S6). As this project opportunistically collected satellite data when strandings were reported, we also had no methodological control over the way local ground data were collected and reported (see supplemental S6). However, the broader patterns identified here in terms of how environment, image resolution and cetacean size impact detection are consistent across stranding events.

In remote regions without ground-based validation opportunities, alternative validation methods could be explored to assist detection. For example, multispectral information could be used to confirm carcass detections if spectral signatures are distinct from confounding features.

4.2. *VHR optical satellite imagery: minimum spatial resolution*

For large stranded odontocete and similar sized target features, like baleen whales, 100% agreement with the ground count and median certainty agreement of sperm whales counts, at both 0.5 and 0.3 m spatial resolution, demonstrated that 0.5 m spatial resolution imagery is suitable for monitoring. The high level of morphological detail at both resolutions enables confident identification based on the whales' size, distinct cetacean features (*e.g.*, ellipsoid shape and visible fluke), and contrast with the surrounding environment (Fig. 4). This finding aligns with previous studies identifying whales from space, where both live and stranded baleen whales have been successfully detected and counted in 0.5 m imagery (Fretwell et al., 2014; Fretwell et al., 2019).

For counting smaller odontocete species, agreement with the ground count and median certainty agreement at 0.5 m spatial resolution was high under ideal imaging conditions. The improvement in agreement at 0.3 m spatial resolution was substantial, as expected given the higher level of detail. At 0.15 m spatial resolution, observer agreement with the ground count revealed near 100% accuracy, with only a 0.2% overcount (6 individuals) in optimal conditions. Along with the 92% median certainty agreement, 0.15 m imagery holds promise for achieving highly accurate counting. However, a detailed comparison of observer 1 and 2's definite and likely detections at 0.15 m and 0.3 m resolutions revealed minimal differences. Observer 1 detected four additional individuals and observer 2 detected three more at 0.15 m compared to 0.3 m. Both observers made fewer definite and more possible detections at 0.15 m spatial resolution. This, together with the marginal increase in median certainty agreement, suggests that artifacts are introduced during the artificial 'uplift' process and may not accurately represent real-world conditions on the ground. Cubaynes et al., (2024) and Yalcin et al., (2021) reported similar artifact-related discrepancies in 0.15 m VHR optical satellite imagery, which resulted in lower counting accuracies of walruses. While native resolution provided the closest fit to ground counts in some instances (two images), this was not always the case. For instance, when resolution was 'uplifted' from 0.5 m to 0.3 m, observer counts improved for one image but declined for another. Further investigation is needed to determine the conditions in which 'uplift' might improve accuracy relative to native resolution. Additionally, it is important to acknowledge the limited control users have in the replicability of 'uplifted' products, as methodological developments could result in a different product even when ordering the same imagery used in this study. The launch of Albedo, a constellation of VHR optical satellite imaging sensors capable of capturing Earth at 0.1 m native spatial resolution (Albedo, 2025), is expected to enable highly accurate and confident counts of small odontocete strandings (Cubaynes et al., 2024). Given the minimal difference in count accuracy and certainty between 0.15 m and 0.3 m imagery, and the significant difference in costs, 0.3 m imagery is recommended for counting small-bodied odontocete strandings in ideal conditions, with 0.5 m serving as a viable alternative when higher resolutions are unavailable. Under suboptimal conditions, access to the highest available native spatial resolution available is advised. If the purpose of a study or monitoring programme is solely detection, 0.5 m imagery remains sufficient for small stranded odontocetes. For example, in remote regions where there is little to no information on strandings, even knowing an event has happened through satellite observations would be highly valuable.

4.3. SAR satellite imagery: detection and count

This study presents the first published detection and count of cetaceans in SAR. While evidence of cetacean presence in the form of a wake (Radford et al., 1994) and inferences of distribution in North Atlantic right whale (*Eubalaena australis*), based on variation in physical indexes, such as sea surface roughness (Perrie et al., 2023), have been inferred using SAR, no published study has detected a cetacean itself. From existing knowledge of global climate and cloud cover (see NASA's global cloud fraction visualisations (NASA Earth Observatory, 2024)), New Zealand is cloudy (Aotearoa, the Māori name for New Zealand, means 'long white cloud' (An Encyclopaedia of New Zealand, 1966)), with an annual average (1961–1990) cloud cover of 63.8% (Osborn, 2016). Based on the dielectric constant of cetaceans compared with their surrounding environment and changes in surface roughness associated with stranding events, SAR could be a solution for monitoring strandings in New Zealand and other regions impacted by high cloud cover. On average the optical satellite data used in this study was acquired approximately ~six days after the event and direct counts, underscoring the challenge of real-time monitoring. In conjunction with the diminished agreement between counts in cloudy conditions reported here, it is apparent cloud is a significant challenge for establishing long-term stranding monitoring programmes using optical satellites.

Analysis of X-band TerraSAR-X imagery revealed strong backscatter signals from stranded cetaceans, appearing bright (with even tyre tracks from the response team visible from space; Fig. 7b), as previously reported for walruses (Fischbach and Douglas, 2021). However, there was low agreement between observers reviewing SAR imagery. This could be due to observers' first exposure to SAR imagery, the effect of restricting observer access to an optical comparison for validation of their detections, and/or the presence of confounding features (*e.g.,* rocks, non-organic marine debris, and some species of macroalgae (Hadjal et al., 2025)). Fischbach and Douglas (2021) attributed their successful application of SAR to detect walruses to the homogenous environment, a fine sandy beach with uniform terrain. In contrast, in the matched optical image in our study a high algal presence was observed, which sometimes returned sufficient backscatter to confound carcass detection (Fig. 10).

We found that certain carcasses visible in the optical image were sometimes absent in the SAR image (Fig. 7) or exhibited a weak signal in the SAR image, similar to algae (Fig. 10b). Potential explanations include: (1) orientation differences between carcasses and SAR collection polarisation (the orientation the electromagnetic radar wave oscillates), though this could not be tested as only HH-(Horizontal transmit) polarised imagery was available; (2) incidence angle of the collection (>30°, at oblique angles smooth specular surfaces, like cetacean epidermis and blubber, can exhibit a weaker backscatter); (3) carcasses being washed offshore between SAR and optical acquisitions; (4) carcasses being partially buried by sand; or (5) misidentification of algae as stranded cetaceans in the matched optical image, which then appeared to be missing or less bright in the SAR imagery. The first explanation is less likely as polarisation was found to not impact the backscatter of walruses (Fischbach et al., 2025; Fischbach and Douglas, 2021), however, further investigation should be undertaken into the impacts of carcass orientation in SAR. If the latter is correct, the distinct biological, chemical, and physical properties of algae may result in weaker SAR backscatter, suggesting that SAR might be useful in eliminating confounding features in optical imagery. In our pilot study, we found that the effect of algae on detections of stranded cetaceans in SAR was inconclusive, and could have contributed to the low agreement. Therefore, we recommend future studies to employ image differencing before and after strandings to provide further insight into the role of SAR in distinguishing confounding features.

Despite the low agreement between observers in SAR, if only comparing the total features identified by two or more observers in the shared cloud-free regions between the SAR and matched optical satellite image (Table 1), observers achieved similar counts. By including only those detections made by more than one observer, and/or detections assigned high certainty (definite and likely), SAR could potentially achieve high count accuracy.

In summary, SAR shows promise for confirming stranding events in remote and cloudy regions and to estimate event magnitude where field access is limited. With continued refinement, SAR has the potential to be used as a standalone tool in absence of optical imagery/direct counts, when applied by local experts in well mapped regions. However, at least in this initial testing phase of SAR, without matched optical imagery/direct counts for validation, confirming detections and substantiating counts remains challenging. More pilot studies of SAR are needed across various environments and species to assess viability for monitoring cetacean strandings, with matched optical imagery and direct counts to assist validation.

In remote coastal areas, SAR imagery could complement optical image acquisitions, to help flag areas of concern, gather baseline information and aid more rapid response. However, we note that scaling this tool up will be expensive with the current available satellites. High spatial resolution SAR data, like TerraSAR-X's staring spotlight mode used in this study, capture a small surface area per image (approximately 5 by 5 km). Scaling SAR acquisitions to monitor large coastal areas, potentially at repeated intervals, may be cost prohibitive for strandings networks, particularly in coastal areas with limited economic resources, and thus image accessibility needs to be increased (see supplemental S6). Further research, including improved observer training and acquisitions before, during and after an event to help distinguish confounding features from new stranding events, will be necessary to refine SAR's application for cetacean stranding detection and monitoring.

4.4. Future work

This study focused on regions where satellite detections could be validated with direct counts. Further work should aim to capture and

Fig. 11. Images 1–4 correspond to event numbers in section 'Area of Study' and Fig. 2, and all imagery metadata is available in supplemental S2. All VHR optical satellite imagery are 0.5 m spatial resolution and all PlanetScope optical satellite imagery are 3 m spatial resolution. (1.a) Pleiades VHR image collected 28 November 2018, of the Stewart Island long-finned pilot whale (LFPW) mass stranding event (MSE), and (1.b) PlanetScope image of the same event captured on the same day. (2.a) PlanetScope image of the King Island sperm whale MSE collected 19 September 2022, the date of the stranding event, (2.b) GeoEye-1 VHR image collected 28 September 2022, of the same event, and (2.c) PlanetScope image of the same MSE captured 30 September 2022, two days after the VHR image. (3(a).a) GeoEye-1 VHR image collected 14 October 2022, of the Maunganui Beach, Chatham Island LFPW MSE, and (3(a).b) PlanetScope image of the same event captured on the same day. (3(b).a) WorldView-3 VHR image collected 5 October 2023, of the Long Beach, Chatham Island LFPW MSE, and (3(b).b) PlanetScope image of the same event captured on the same day (individual animals not detectable). (4.a) PlanetScope image of the Pitt Island LFPW MSE collected 10 October 2022, the date of the stranding event, (4.b), PlanetScope image of the same MSE captured 19 October 2022, two days before VHR image, and (4.c) WorldView-2 VHR image collected 21 October 2022 of the same MSE.

trial satellite imagery for smaller stranded delphinid species, to determine the smallest feature that can be reliably detected and counted. Given the uncertainty of strandings events, tackling specific questions necessary to refine the tool (like the smallest species detectable) may be challenging. The experimental design of Ponti et al., (2025) to use decoy carcasses, could form an effective method to troubleshoot monitoring of strandings by satellites. Ponti et al., (2025), investigated detection rates of different monitoring methods (*i.e.*, drone and visual observations made from a vessel, vehicle, and on foot), for decoy carcasses deployed in varying marine environments. They found that drones, which share a similar look angle to satellites were more effective at detecting decoys than conventional methods for monitoring strandings. Repeating Ponti et al., (2025) approach to include satellites, could be a robust method to compare how satellites perform within the current suite of tools for monitoring strandings.

All features here were manually detected, which is time consuming and subject to observer bias. The dataset generated here is the largest dataset of stranded cetaceans in satellite imagery in the world (Clarke et al., 2025b), and provides a starting point to develop machine learning tools to speed and scale up detection and counting of cetacean strandings from space. Furthermore, a method of automation that could help reduce costs, is the development of an initial detector using lower cost coarser spatial resolution optical satellite data. For example, developing a change detector (identifying changes in spectra) using 3 m PlanetScope imagery (continuous collection capabilities and daily revisits to the same location on Earth), to scan large (suspected) high risk remote coastal areas. Such a tool could help to flag areas of concern/highlight an unfolding event to stranding managers, inform on-ground response, or help direct funds for investment in VHR optical and SAR satellite imagery to quantify an event. Developing an automated change detector would first need the accuracy and limitations of PlanetScope data to be understood. An initial visualisation of matched/close in time PlanetScope imagery to the MSE's studied here, evidences the potential of lower cost high spatial resolution satellite imagery for monitoring the occurrence of large-bodied whale strandings, or tightly packed large stranding events of smaller-bodied whale and dolphin species (see Fig. 11 and Table S2.2 in supplemental S2 for PlanetScope imagery metadata).

Satellites could also be valuable in evaluating the impact of large-scale emerging diseases, for example, die-offs resulting from avian influenza for species around New Zealand and remote sub-Antarctic Islands, where impacts may go unnoticed (Bamford et al., 2025; Banyard et al., 2024; Runstadler and Puryear, 2020; Waller et al., 2025).

Changes in spectral signatures through various phases of decomposition could also be used as a proxy to estimate the stage of decay and time of the stranding event, and aid information provision to stranding networks where it is not possible to visit the stranding (*i.e.,* remote and complex coastal regions).

In the early application of satellite-based monitoring of stranding events, continued testing of VHR optical and SAR satellite imagery in accessible coastal regions with adequate direct counts made by local agencies and conservation groups, will be necessary to make the tool reliable. For integration of satellite-based monitoring into stranding networks, robust evaluation metrics to determine whether satellites are the most cost-effective solution are required. For example, the trade-off of reliability, speed, and expense of deploying ground or aerial surveys compared with satellite-based surveys in hard-to-reach coastal regions, considering also satellite revisit rates and cloud cover (Clarke et al., 2025a).

5. Conclusions and recommendations

VHR optical satellite imagery is an effective tool for detecting and counting both large and small odontocete species, given favourable environmental conditions (little to no cloud, highly contrasting environment to the target feature, image collection close to nadir, and few to no confounding features). To optimise cost-efficiency, 0.3 m is recommended for the detection and count of smaller odontocetes and 0.5 m for larger odontocete and mysticetes. Selecting observers with target feature experience and robust training is key to achieving high accuracy datasets. Further pilot studies using SAR should be conducted to further explore its utility in ideal conditions, with few to no confounding features. SAR has the potential to complement strandings monitoring in remote regions *via* nocturnal observations as well as in regions with persistent cloud cover, increasing the likelihood of real-time event detection and emergency response to events as they unfold. Together, VHR optical and SAR satellites can enhance the capacity of networks to monitor strandings in hard-to-reach coastal areas with limited resources. This research would not have been possible without the support of local researchers; if we can continue to refine the tool and work towards more equitable access, satellites could help stranding networks, worldwide, to get closer to achieving their long-term monitoring and conservation goals.

CRediT authorship contribution statement

Penny J. Clarke: Writing – review & editing, Writing – original draft, Visualization, Validation, Methodology, Investigation, Funding acquisition, Formal analysis, Data curation, Conceptualization. **Hannah C. Cubaynes:** Writing – review & editing, Visualization, Validation, Supervision, Methodology, Investigation, Data curation. **Karen A. Stockin:** Writing – review & editing, Validation, Supervision, Methodology, Investigation. **Ellen Bowler:** Writing – review & editing, Validation, Methodology, Investigation, Formal analysis, Data curation. **Kris Carlyon:** Writing – review & editing, Investigation. **Marie R.G. Attard:** Writing – review & editing, Methodology, Data curation. **Peter T. Fretwell:** Writing – review & editing, Supervision. **Aliaksandra Skachkova:** Writing – review & editing, Validation, Methodology. **Asha de Vos:** Writing – review & editing, Supervision. **Kaitlin M. McConnell:** Writing – review & editing, Validation, Methodology. **Encarni Medina-Lopez:** Writing – review & editing, Supervision. **Sergio Lopez Dubon:** Writing – review & editing. **Jennifer A. Jackson:** Writing – review & editing, Visualization, Validation, Supervision, Methodology, Funding acquisition, Data curation.

Declaration of competing interest

The authors declare that they have no known competing financial interests or personal relationships that could have appeared to influence the work reported in this paper.

Acknowledgements

This study represents a contribution to the Ecosystems programme at the British Antarctic Survey Polar Science for Planet Earth Programme, funded by the Natural Environment Research Programme. This research has been supported by the Natural Environment Research Council (NERC) through a SENSE CDT studentship (grant no. NE/T00939X/1). We are grateful for additional financial support provided through, the British Antarctic Survey (BAS) Innovation Voucher, Sentinel Hub and their #30MapChallenge competition, and BAS Ecosystems. We are thankful to the support and cooperation of Vantor (formerly Maxar Technologies Ltd; Emma Meheux and Paulo Godhino) and Airbus (Katherine Elsom, Peter Buchanan, Gregory Richardson, and Sheena White) for their rapid response and efforts to enable successful collection of the imagery analysed here. Additionally, we are thankful to the Department of Conservation, New Zealand, the Tasmanian Government's Department of Natural Resources and Environment Tasmania, and Tamzin Henderson, for their generosity to support this study with vital ground and aerial data.

Appendix A. Supplementary data

Supplementary data to this article can be found online at https://doi.org/10.1016/j.ecoinf.2026.103924.

Data availability

Stranded cetacean features detected and annotated by all observers are available to download open-access at the British Antarctic Survey Polar Data Centre (doi:10.5285/b26c3a3d-73c8-4500-9a23-696011c20a45; Clarke et al., 2025b). Due to licencing agreements, satellite images are not shared here, however, the full metadata of all satellite imagery used are provided in supplemental S2. Full methodological details including workflows, code, and information necessary to access and reproduce the image-pre-processing steps are openly available in Clarke et al., (2026a) and on Zenodo at: doi:10.5281/zenodo.20547057 (Clarke et al., 2026b), with the most up-to-date version found at: https://github.com/PennyJClarke/strandings_from_space).

References

Abileah, R., 2002. Marine mammal census using space satellite imagery. U.S. Navy J. Underwater Acoustics 52 (3), 709–724.

Albedo, 2025. Albedo. Available from: https://albedo.com/ (Accessed: April 8, 2025).

An Encyclopaedia of New Zealand, 1966. AOTEAROA. Available from: https://teara.govt.nz/en/1966/aotearoa (Accessed: April 17, 2025).

Aniceto, A.S., Tassara, L., Rikardsen, A., Blévin, P., 2021. Mass strandings of seven toothed and baleen whale species in northern Norway in March 2020 call for further investigation. Polar Biol. 44, 1457–1461. https://doi.org/10.1007/s00300-021-02869-6. Available at:

Attard, M.R.G., Phillips, R.A., Bowler, E., Clarke, P.J., Cubaynes, H., Johnston, D.W., Fretwell, P.T., 2024. Review of satellite remote sensing and unoccupied aircraft systems for counting wildlife on land. Remote Sens. 16 (4), 627. https://doi.org/10.3390/rs16040627.

Attard, M.R.G., Phillips, R.A., Oppel, S., Bowler, E., Fretwell, P.T., 2025. Feasibility of using very high-resolution satellite imagery to monitor Tristan albatrosses *Diomedea dabbenena* on Gough Island. Endanger. Species Res. 56, 187–199. https://doi.org/10.3354/esr01396. Available at:

Bamford, C., Kelly, N., Dalla Rosa, L., Cade, D., Cubaynes, H., Mesquita, A., Gerrish, L., Friedlaender, A., Jackson, J., 2020. A comparison of baleen whale density estimates derived from overlapping satellite imagery and a shipborne survey. Sci. Rep. 10, 12985. https://doi.org/10.1038/s41598-020-69887-y.

Bamford, C.C.G., Fenney, N., Coleman, J., Fox-Clarke, C., Dickens, J., Fedak, M., Fretwell, P., Hückstädt, L., Hollyman, P., 2025. Highly pathogenic avian influenza viruses (HPAIV) associated with major southern elephant seal decline at South Georgia. Commun. Biol. 8, 1493. https://doi.org/10.1038/s42003-025-09014-7.

Banyard, A.C., Bennison, A., Byrne, A.M.P., Reid, S.M., Lynton-Jenkins, J.G., Mollett, B., De Silva, D., Peers-Dent, J., Finlayson, K., Hall, R., Blockley, F., Blyth, M., Falchieri, M., Fowler, Z., Fitzcharles, E.M., Brown, I.H., James, J., 2024. Detection and spread of high pathogenicity avian influenza virus H5N1 in the Antarctic region. Nat. Commun. 15, 7433. https://doi.org/10.1038/s41467-024-51490-8.

Betty, E.L., Bollard, B., Murphy, S., Ogle, M., Hendriks, H., Orams, M.B., Stockin, K.A., 2020. Using emerging hot spot analysis of stranding records to inform conservation management of a data-poor cetacean species. Biodivers. Conserv. 29, 643–665. https://doi.org/10.1007/s10531-019-01903-8. Available at:

Betty, E.L., Stockin, K.A., Hinton, B., Bollard, B.A., Smith, A.N.H., Orams, M.B., Murphy, S., 2022. Age, growth, and sexual dimorphism of the southern hemisphere long-finned pilot whale (*Globicephala melas edwardii*). J. Mammal. 103 (3), 560–575. https://doi.org/10.1093/jmammal/gyab165. Available at:

Betty, E.L., Stockin, K.A., Hinton, B., Bollard, B., Orams, M.B., Murphy, S., 2023. Age- and sex-specific survivorship of the southern hemisphere long-finned pilot whale (*Globicephala melas edwardii*). J. Mammal. 104 (1), 39–48. https://doi.org/10.1093/jmammal/gyac085. Available at:

Bird, C.N., Dawn, A.H., Dale, J., Johnston, D.W., 2020. A semi-automated method for estimating Adélie penguin colony abundance from a fusion of multispectral and thermal imagery collected with unoccupied aircraft systems. Remote Sens. 12 (22), 3692. https://doi.org/10.3390/rs12223692.

Boulent, J., Charry, B., Kennedy, M.M., Tissier, E., Fan, R., Marcoux, M., Watt, C.A., Gagné-Turcotte, A., 2023. Scaling whale monitoring using deep learning: a human-in-the-loop solution for analyzing aerial datasets. Front. Mar. Sci. 10, 1099479. https://doi.org/10.3389/fmars.2023.1099479.

Brabyn, M.W., McLean, I.G., 1992. Oceanography and coastal topography of herd-stranding sites for whales in New Zealand. J. Mammal. 73 (3), 469–476. https://doi.org/10.2307/1382012. Available at:

Charry, B., Tissier, E., Iacozza, J., Marcoux, M., Watt, C.A., 2021. Mapping Arctic cetaceans from space: a case study for beluga and narwhal. PLoS One 16 (8), e0254380. https://doi.org/10.1371/journal.pone.0254380.

Clarke, P.J., Cubaynes, H.C., Stockin, K.A., Olavarría, C., de Vos, A., Fretwell, P.T., Jackson, J.A., 2021. Cetacean strandings from space: challenges and opportunities of very high resolution satellites for the remote monitoring of cetacean mass strandings. Front. Mar. Sci. 8, 650735. https://doi.org/10.3389/fmars.2021.650735.

Clarke, P.J., Cubaynes, H.C., Jackson, J.A., Taylor, N.L., Johnston, D.W., de Vos, A., Fretwell, P.T., Skachkova, A., Jones, G., 2025a. Talking about the weather: the feasibility of using very high-resolution optical satellite imagery to monitor live and stranded cetaceans around the UK and UK overseas territories. Mar. Mamm. Sci., e70074 https://doi.org/10.1111/mms.70074.

Clarke, P.J., Cubaynes, H.C., Bowler, E., Jackson, J.A., Attard, M.R.G., Stockin, K.A., Carlyon, K., 2025b. Point Annotation Dataset of Stranded Whale and Dolphin Species Identified in Very High-resolution Optical and SAR Satellite Imagery along Offshore Islands of New Zealand and Tasmania between 2018-2023. NERC EDS UK Polar Data Centre. https://doi.org/10.5285/b26c3a3d-73c8-4500-9a23-696011c20a45.

Clarke, P.J., Cubaynes, H.C., Stockin, K.A., Bowler, E., Carlyon, K., Attard, M.R.G., Fretwell, P.F., Skachkova, A., de Vos, A., McConnell, K.M., Medina-Lopez, E., Lopez Dubon, S., Jackson, J.A., 2026a. Open-source satellite image pre-processing and annotation workflows: stranded whale and dolphin case study. MethodsX. https://doi.org/10.1016/j.mex.2026.103949.

Clarke, P.J., Cubaynes, H.C., Stockin, K.A., Bowler, E., Carlyon, K., Attard, M.R.G., Fretwell, P.T., Skachkova, A., de Vos, A., McConnell, K.M., Medina-Lopez, E., Lopez Dubon, S., Jackson, J.A., 2026b. Strandings_from_space (v1.0.0). Zenodo. https://doi.org/10.5281/zenodo.20547057.

Coombs, E.J., Deaville, R., Sabin, R.C., Allan, L., O'Connell, M., Berrow, S., Smith, B., Brownlow, A., Ten Doeschate, M., Penrose, R., Williams, R., Perkins, M.W., Jepson, P.D., Cooper, N., 2019. What can cetacean stranding records tell us? A study of UK and Irish cetacean diversity over the past 100 years. Mar. Mamm. Sci. 35 (4), 1527–1555. https://doi.org/10.1111/mms.12610. Available at:

Corrêa, A.A., Quoos, J.H., Barreto, A.S., Groch, K.R., Eichler, P.P.B., 2022. Use of satellite imagery to identify southern right whales (*Eubalaena australis*) on a Southwest Atlantic Ocean breeding ground. Mar. Mamm. Sci. 38 (1), 87–101. https://doi.org/10.1111/mms.12847. Available at:

Cubaynes, H.C., Fretwell, P.F., Bamford, C., Gerrish, L., Jackson, J.A., 2019. Whales from space: four mysticete species described using new VHR satellite imagery. Mar. Mamm. Sci. 35 (2), 466–491. https://doi.org/10.1111/mms.12544. Available at:

Cubaynes, H.C., Clarke, P.J., Goetz, K.T., Aldrich, T., Fretwell, P.T., Leonard, K.E., Khan, C.B., 2023. Annotating very high-resolution satellite imagery: a whale case study. MethodsX 10, 102040. https://doi.org/10.1016/j.mex.2023.102040.

Cubaynes, H.C., Forcada, J., Kovacs, K.M., Lydersen, C., Downie, R., Fretwell, P.T., 2024. Walruses from space: walrus counts in simultaneous remotely piloted aircraft system versus very high-resolution satellite imagery. Remote Sens. Ecol. Conserv. 10 (5), 584–596. https://doi.org/10.1002/rse2.391. Available at:

Eineder, M., Fritz, T., Mittermayer, F.T., Roth, A., Börner, E., Breit, H., Braeutigam, T., K., T., 2013. TerraSAR-X Ground Segment Basic Product Specification Document. Doc: TX-GS-DD-3302. German Aerospace Center (DLR), Bonn, Germany, pp. 1–126. Available at: https://sss.terrasar-x.dlr.de/docs/TX-GS-DD-3302.pdf (Accessed: April 23, 2026).

Fischbach, A.S., Douglas, D.C., 2021. Evaluation of satellite imagery for monitoring Pacific walruses at a large coastal haulout. Remote Sens. 13 (21), 4266. https://doi.org/10.3390/rs13214266.

Fischbach, A.S., Taylor, R.L., Douglas, D.C., 2025. Monitoring Pacific walrus coastal haulouts by satellite to estimate herd abundance and distribution. Wildl. Soc. Bull. 49 (4), e1614. https://doi.org/10.1002/wsb.1614.

Fretwell, P.T., Staniland, I.J., Forcada, J., 2014. Whales from space: counting southern right whales by satellite. PLoS One 9 (2), e88655. https://doi.org/10.1371/journal.pone.0088655.

Fretwell, P.T., Scofield, P., Phillips, R.A., 2017. Using super-high resolution satellite imagery to census threatened albatrosses. Ibis 159 (3), 481–490. https://doi.org/10.1111/ibi.12482. Available at:

Fretwell, P.T., Jackson, J.A., Ulloa Encina, M.J., Häussermann, V., Perez Alvarez, M.J., Olavarría, C., Gutstein, C.S., 2019. Using remote sensing to detect whale strandings in remote areas: the case of sei whales mass mortality in Chilean Patagonia. PLoS One 14 (11), e0225209. https://doi.org/10.1371/journal.pone.0222498.

Geraci, J.R., Loundsbury, V.J., 2005. Marine mammal ashore: a field guide for strandings, 2nd ed. National Aquarium in Baltimore, Inc., Baltimore.

Gulland, F.M.D., Asmutis-Silvia, R., Boehm, J., DiGiovanni Jr., R.A., Goertz, C.E.C., Huggins, J.L., Lovewell, G.N., Moore, K.M., West, K., 2025. Marine mammal stranding networks in the 21st century: whence and whither? Mar. Mamm. Sci. 41 (3), e70016. https://doi.org/10.1111/mms.70016.

Hadjal, M., Barnes, B.B., Hu, C., Qi, L., Papageorgiou, D., Topouzelis, K., 2025. Detection potential of floating matter in high-resolution X-band SAR data: initial results with visual interpretations. Front. Remote Sens. 6, 1693286. https://doi.org/10.3389/frsen.2025.1693286.

Hamilton, L.J., 2018. Large mass strandings of selected odontocete species: statistics, locations, and relation to earth processes. J. Cetacean Res. Manag. 19, 57–78. https://doi.org/10.47536/jcrm.v19i1.415. Available at:

Häussermann, V., Gutstein, C.S., Bedington, M., Cassis, D., Olavarria, C., Dale, A.C., Valenzuela-Toro, A.M., Perez-Alvarez, M.J., Sepúlveda, H.H., McConnell, K.M., Horwitz, F.E., Försterra, G., 2017. Largest baleen whale mass mortality during strong El Niño event is likely related to harmful toxic algal bloom. PeerJ 5, e3123. https://doi.org/10.7717/peerj.3123/table-7.

Höschle, C., Cubaynes, H.C., Clarke, P.J., Humphries, G., Borowicz, A., 2021. The potential of satellite imagery for surveying whales. Sensors 21 (3), 963. https://doi.org/10.3390/s21030963.

IWC, 2017. Report of the workshop on investigations of large mortality events, mass strandings and international stranding response. J. Cetacean Res. Manag. 18 (Supplement), 603–614. https://archive.iwc.int/pages/download.php?ref=6409&ext=pdf&alternative=3290&noattach=true.

Jefferson, T.A., Hung, S.K., Robertson, K.M., Archer, F.I., 2011. Life history of the Indo-Pacific humpback dolphin in the Pearl River Estuary, southern China. Mar. Mamm. Sci. 28 (1), 84–104. https://doi.org/10.1111/j.1748-7692.2010.00462.x. Available at:

Khan, C.B., Goetz, K.T., Cubaynes, H.C., Robinson, C., Murnane, E., Aldrich, T., Sackett, M., Clarke, P.J., LaRue, M.A., White, T., Leonard, K., Ortiz, A., Lavista Ferres, J.M., 2023. A biologist guide to the galaxy: leveraging artificial intelligence and very high-resolution satellite imagery to monitor marine mammals from space. J. Mar. Sci. Eng. 11 (3), 595. https://doi.org/10.3390/jmse11030595.

Laborie, J., Authier, M., Chaigne, A., Delord, K., Weimerskirch, H., Guinet, C., 2023. Estimation of total population size of southern elephant seals (*Mirounga leonina*) on Kerguelen and Crozet Archipelagos using very high-resolution satellite imagery. Front. Mar. Sci. 10, 1149100. https://doi.org/10.3389/fmars.2023.1149100.

LaRue, M.A., Rotella, J.J., Garrott, R.A., Siniff, D.B., Ainley, D.G., Stauffer, G.E., Porter, C.C., Morin, P.J., 2011. Satellite imagery can be used to detect variation in abundance of Weddell seals (*Leptonychotes weddellii*) in Erebus Bay, Antarctica. Polar Biol. 34, 1727–1737. https://doi.org/10.1007/s00300-011-1023-0. Available at:

LaRue, M.A., Stapleton, S., Anderson, M., 2017. Feasibility of using high-resolution satellite imagery to assess vertebrate wildlife populations. Conserv. Biol. 31 (1), 213–220. https://doi.org/10.1111/cobi.12809. Available at:

Leeney, R.H., Amies, R., Broderick, A.C., Witt, M.J., Loveridge, J., Doyle, J., Godley, B.J., 2008. Spatio-temporal analysis of cetacean strandings and bycatch in a UK fisheries hotspot. Biodivers. Conserv. 17, 2323–2338. https://doi.org/10.1007/s10531-008-9377-5. Available at:

Lennert-Cody, C.E., Buckland, S.T., Gerrodette, T., Webb, A., Barlow, J., Fretwell, P.T., Maunder, M.N., Kitakado, T., Moore, J.E., Scott, M.D., Skaug, H.J., 2019. Review of potential line-transect methodologies for estimating abundance of dolphin stocks in the eastern tropical Pacific. J. Cetacean Res. Manag. 19, 9–21. Available at: 10.47536/jcrm.v19i1.411.

Lennon, R.L., Williams, R.S., Allan, K.J., ten Doeschate, M.T.I., Davison, N.J., Babayan, S. A., Brownlow, A.C., 2025. An approach to using stranding data to monitor cetacean population trends and guide conservation strategies. Sci. Rep. 15, 28417. https://doi.org/10.1038/s41598-025-12928-1.

McMahon, C.R., Howe, H., van den Hoff, J., Alderman, R., Brolsma, H., Hindell, M.A., 2014. Satellites, the all-seeing eyes in the sky: counting elephant seals from space. PLoS One 9 (3). https://doi.org/10.1371/journal.pone.0092613. Available at.

NASA Earth Observatory, 2024. Cloud Fraction. Available from: https://earthobservatory.nasa.gov/global-maps/MODAL2_M_CLD_FR (Accessed: July 24, 2024).

Osborn, T., 2016. Climate information for New Zealand: climate observations - cloud cover. Available from: https://crudata.uea.ac.uk/~timo/climgen/national/web/NewZealand/obs_cld.htm (Accessed: June 08, 2025).

Perrie, W., Shen, H., Tao, J., Danielson, R., 2023. A physical index towards real time monitoring of potential whale habitats from space in Canadian Technical Report of Fisheries and Aquatic Sciences. Fisheries and Oceans Canada, p. 35. Available at: https://publications.gc.ca/collections/collection_2023/mpo-dfo/Fs97-6-3533-eng.pdf.

Perrin, W.F., Geraci, J.R., 2009. Stranding. In: Perrin, W.F., Würsig, B., Thewissen, J.G. M. (Eds.), Encyclopedia of Marine Mammals, Second edition. Academic Press, pp. 1118–1123.

Planet Labs, 2025. Sentinel hub. Available from: https://www.sentinel-hub.com/ (Accessed: March 11, 2022).

Platonov, N., Mordvintsev, I.N., Rozhnov, V.V., 2013. The possibility of using high resolution satellite images for detection of marine mammals. Biol. Bull. 40 (2), 217–226. https://doi.org/10.1134/S1062359013020106. Available at:

Ponti, M.J., Russell, M.L., Díaz Clark, C., Cloyed, C.S., Carmichael, R.H., Johnson, C.L., Bloodgood, J.C.G., 2025. Stranded marine mammal detection by the public, trained responders, and drones using decoy carcasses. Mar. Mamm. Sci. 41 (1), e13169. https://doi.org/10.1111/mms.13169.

Pyenson, N., 2011. The high fidelity of the cetacean stranding record: insights into measuring diversity by integrating taphonomy and macroecology. Proc. Biol. Sci. 278, 3608–3616. https://doi.org/10.1098/rspb.2011.0441.

Radford, S.F., Gran, R.L., Miller, R.V., 1994. Detection of whale wakes with synthetic aperture radar. Mar. Technol. Soc. J. 28 (2), 46–52.

Rees, W.G., 2013. Physical Principles of Remote Sensing, 3rd ed. Cambridge University Press, Cambridge.

Roman, J., Estes, J.A., Morissette, L., Smith, C., Costa, D., McCarthy, J., Nation, J.B., Nicol, S., Pershing, A., Smetacek, V., 2014. Whales as marine ecosystem engineers. Ecol. Soc. Am. Front. Ecol. Environ. 12 (7), 377–385. https://doi.org/10.1890/130220.

Runstadler, J.A., Puryear, W., 2020. A brief introduction to influenza a virus in marine mammals, in animal influenza virus: methods and protocols, E. Spackman, Editor. Springer US, New York, NY, pp. 429–450.

Stapleton, S., LaRue, M.A., Lecomte, N., Atkinson, S., Garshelis, D., Porter, C., Atwood, T., 2014. Polar bears from space: assessing satellite imagery as a tool to track Arctic wildlife. PLoS One 9 (7), e101513. https://doi.org/10.1371/journal.pone.0101513.

Stockin, K.A., Binedell, V., Wiseman, N., Brunton, D.H., Orams, M.B., 2009. Behavior of free-ranging common dolphins (*Delphinus sp.*) in the Hauraki Gulf, New Zealand. Mar. Mamm. Sci. 25 (2), 283–301. https://doi.org/10.1111/j.1748-7692.2008.00262.x. Available at:

Vantor, 2020. Seeing the world with complete clarity at 15 cm HD resolution. Available from: https://vantor.com/blog/seeing-the-world-with-complete-clarity-at-15-cm-hd-resolution/ (Accessed: April 21, 2026).

Vantor, 2025. Discover. Available from: https://xpress.maxar.com/ (Accessed: October 24, 2025).

Waller, S.J., Wierenga, J.R., Heremia, L., Darnley, J.A., de Vries, I., Dubrulle, J., Robinson, Z., Miller, A.K., Niebuhr, C.N., Melville, D.S., Schuckard, R., Battley, P.F., Wille, M., Alai, B., Cole, R., Cooper, J., Ellenberg, U., Elliott, G., Faulkner, J., Fischer, J.H., Hay, L., Houston, D., Keys, B.C., Long, J., Long, R., Mattern, T., McNutt, L., Moore, P., Neil, O., Osborne, J., Pagé, A.-S., Parker, K.A., Perry, M., Philp, B., Rexer-Huber, K., Russell, J.C., Sagar, R., Ruru, T.T., Thompson, T., Thomson, L., Tinnemans, J., Uddstrom, L., Waipoua, T.A., Walker, K., Whitehead, E., Wickes, C., Young, M.J., Winter, D., McInnes, K., Holmes, E.C., Geoghegan, J.L., 2025. Foraging ecology drives viral community structure in New Zealand's aquatic birds. bioRxiv. https://doi.org/10.64898/2025.12.09.693119.

Woodhouse, I.H., 2006. Introduction to microwave remote sensing. CRC Press, Boca Raton.

Yalcin, I., Kocaman, S., Saunier, S., Albinet, C., 2021. Radiometric quality assessment for Maxar HD imagery. In: The International Archives of the Photogrammetry, Remote Sensing and Spatial Information Sciences. XXIV ISPRS Congress, pp. 797–804. https://doi.org/10.5194/isprs-archives-XLIII-B3-2021-797-2021.